Spatial, seasonal, and historical variation of phytoplankton production in Lake Michigan

Katelyn A. Bockwoldt[a,1], Harvey A. Bootsma[a], and Barry M. Lesht[b*]

[a]School of Freshwater Sciences, University of Wisconsin-Milwaukee, 600 East Greenfield Ave, Milwaukee, WI 53204

[b]GDIT, 5555 S. Blackstone Ave, Suite 2, Chicago, IL 60637

[*]Corresponding author: blesht@gmail,com

[1]Current address: Vermont Department of Environmental Conservation, 1 National Life Drive, Montpelier VT 05602

Keywords: photosynthesis, deep chlorophyll layer, nutrient limitation, seston stoichiometry, quagga mussels, Lake Michigan, phytoplankton

Given their role as Editor, Barry Lesht had no involvement in the peer-review of this article and has no access to information regarding its peer-review. Full responsibility for the editorial process for this article was delegated to Michael Twiss.

Abstract

There have been few direct measurements of phytoplankton production made in Lake Michigan since invasive dreissenid mussels became established in the lake. Here we report the results of 64 measurements of phytoplankton primary production made in Lake Michigan during 2016 and 2017. We conducted two lake-wide surveys, one in the spring 2016 isothermal period and one after summer stratification in 2017 and examined seasonal production with bi-weekly sampling between May and November 2017 at an offshore station in the southwestern part of the lake. We assessed nearshore-offshore gradients by sampling at three transect locations on three occasions in 2017. Spring 2016 production and production:biomass (P:B) ratios (reflective of growth rates) were similar across the lake and were higher than those reported before dreissenid mussels became established, suggesting that despite decreases in phytoplankton biomass, growth rates remain high. Summer 2017 production and growth rates increased from south to north. Areal production in 2017 peaked in late summer. Mean 2017 summer production (499 ± 129 mg C m^{-2} day^{-1}) was lower than values reported prior to the mussel invasion, and the fraction of total production occurring in the deep chlorophyll layer was about half that measured pre-mussels. At the offshore site picoplankton accounted for almost 50% of the chlorophyll. As spring P:B ratios have increased and summer P:B and seston carbon:phosphorus ratios have not changed, we conclude that the decrease in phytoplankton production in Lake Michigan is due primarily to grazing by mussels rather than to stronger nutrient limitation.

Keywords: photosynthesis, deep chlorophyll layer, nutrient limitation, seston stoichiometry, quagga mussels, Lake Michigan, phytoplankton

Introduction

In recent years there appear to have been significant declines in Lake Michigan chlorophyll *a* concentrations, phytoplankton biomass, and phytoplankton production (Fahnenstiel et al., 2010, 2016; Pothoven and Fahnenstiel, 2013; Warner and Lesht, 2015; Yousef et al., 2014). Water clarity and euphotic zone depth have increased (Barbiero et al., 2012; Binding et al., 2015; Yousef et al., 2017; Bunnell et al., 2021) and offshore total phosphorus (TP) concentration has declined significantly since the 1980s (Mida et al., 2010; Dove and Chapra, 2015). This trend toward oligotrophication of Lake Michigan may have negative consequences for higher trophic levels, including declines in zooplankton and fish biomass (Barbiero et al., 2019; Bunnell et al., 2018; Madenjian et al., 2015; Vanderploeg et al., 2012).

The physical, chemical, and biological changes in Lake Michigan generally have been attributed to the effects of invasive dreissenid mussels, particularly the quagga mussel (*Dreissena rostriformis bugensis*) (Hecky et al., 2004; Mosley and Bootsma, 2015; Rowe et al., 2015) though reductions in external phosphorus loading (Chapra and Dolan, 2012) and changes in climate (Warner and Lesht, 2015) may also have had an effect. Observed declines in chlorophyll concentrations and production have been greatest during spring isothermal mixing when mussels have access to phytoplankton in the entire water column (Fahnenstiel et al., 2010), and the historical spring diatom bloom has nearly disappeared (Vanderploeg et al., 2010). Declines in productivity have been less pronounced during summer stratification (Fahnenstiel et al., 2010) when thermal stratification may limit profundal mussels' access to phytoplankton in the euphotic zone.

Although several studies have documented recent changes in phytoplankton production and community composition (Carrick et al., 2015; Reavie et al., 2014; Fahnenstiel et al., 2010),

we have a limited understanding of the spatial and seasonal variation of phytoplankton production in Lake Michigan. Recent measurements of the spatial variability of phytoplankton production in Lake Michigan come from remote sensing studies (Fahnenstiel et al., 2016; Shuchman et al., 2013) rather than from in situ studies. In the absence of ice and cloud cover, remote sensing can provide daily lake-wide estimates of phytoplankton abundance. Remote sensing production models, however, have several limitations, including the inability to account for vertical heterogeneity (Fahnenstiel et al., 2016), difficulty resolving nearshore values (Lee et al., 2015), and uncertainty regarding the conversion of remotely measured signals to phytoplankton biomass, and phytoplankton biomass to primary production rates.

Most published seasonal in situ measurements of phytoplankton production in Lake Michigan come from studies conducted prior to the offshore proliferation of dreissenid mussels (Cuhel and Aguilar, 2003; Fahnenstiel et al., 1989; Fahnenstiel and Carrick, 1988; Fahnenstiel and Scavia, 1987a, b; Scavia et al., 1988; Scavia and Fahnenstiel, 1987). These studies provided valuable insights into phytoplankton dynamics in relation to nutrient loading, zooplankton dynamics, and the top-down influence of planktivorous fishes (Scavia et al., 1988). Recent lower food web changes in Lake Michigan, however, suggest the seasonal dynamics of phytoplankton production have changed since the mussel invasion, but there has only been one published experimental study (Fahnenstiel et al., 2010) and two remote sensing studies (Fahnenstiel et al., 2016; Warner and Lesht, 2015) of post-dreissenid seasonal variability of phytoplankton production in Lake Michigan.

Considering the relative dearth of spatial measurements of phytoplankton production in Lake Michigan, the objective of this study was to investigate the current spatial and seasonal variability of phytoplankton production in the lake. Specifically, we (1) investigated south-north

patterns of phytoplankton production during spring isothermal mixing and summer stratification, (2) measured seasonal production from May to November at an offshore site in southwestern Lake Michigan, (3) assessed nearshore-offshore patterns in production in southwestern Lake Michigan, and (4) compared several current photosynthetic and nutrient variables with values measured before dreissenids became established.

Methods

Field operations

The locations of our field stations are shown in Figure 1 and listed in Table 1. Working from the R/V Lake Guardian in spring 2016 (March 26-29, 2016) and summer 2017 (August 2-7, 2017), we collected samples from an augmented subset of the stations visited biannually by the USEPA's annual Water Quality Survey (WQS). Two of these WQS stations (MI23 and MI34), along the N-S axis of the lake, were sampled in both the spring and summer; two other WQS stations (MI17 in the southern basin and MI47 in northern basin) also were sampled in the spring with an additional, non-WQS station (MI-N) added to sample spring conditions in the northern basin. During the summer, three WQS stations (MI11, MI41, and MI52) were added to the common set along with stations located at the mouth of Green Bay (GB1) and along the eastern shore of the Door Peninsula (DC75) to examine possible influences of outflow from Green Bay on the main lake.

To assess the seasonal variability of phytoplankton production, a 75 m deep site (AW75), 16 km northeast of Milwaukee, Wisconsin was sampled from the R/V Neeskay approximately biweekly from May to November 2017. In July, September, and October 2017 we also collected

samples at two additional stations along a nearshore-offshore transect running from north of Milwaukee to Station AW75, where bottom depths were 15 m (AW15) and 45 m (AW45). Profiles of temperature, chlorophyll *a* fluorescence, beam transmittance, and photosynthetically active radiation (PAR) were measured using a Sea-Bird CTD at each site during the whole-lake surveys. In addition to the PAR sensor on the CTD, data from a PAR sensor mounted on the ship's deck house were recorded at 1-minute intervals while the ship was underway. We used a flow-through fluorometer (Seabird WETStar), supplied with lake water continuously pumped from a port in the ship's hull ~ 2 m below the surface, to monitor surface chlorophyll *a* concentration both while underway and when on station. These measurements were sampled at 1Hz and recorded as 1-minute averages. When sampling was conducted from the R/V Neeskay, a similarly equipped CTD was used to measure profiles of temperature, chlorophyll *a*, beam transmittance, and PAR.

Discrete water samples for photosynthesis experiments and nutrient analyses were collected on the R/V Lake Guardian following EPA Standard Operating Procedure (SOP) LG200 (U.S. EPA, 2017). During spring 2016, when the water column was isothermal, samples were collected from 2 m below the surface and from mid-water column depth. In summer 2017, samples were collected from 5-8 m (considered the mid-epilimnion) and the deep chlorophyll layer (DCL) as determined by examination of the CTD fluorescence profile (sub-epilimnion fluorescence maximum). At AW75, water samples were collected from 5 m and at either 25 or 35 m when the water column was unstratified. During stratification, in addition to the 5 m sample, we collected a sample at the depth of the sub-thermocline fluorescence maximum which was determined by monitoring the real-time CTD display. In October the second depth sampled was either at the base of the epilimnion as determined by the real-time CTD temperature profile,

or the depth of the metalimnetic dissolved oxygen percent saturation maximum, whichever was deeper. Photosynthesis incubation experiments and filtration for nutrient analyses began within 3 hours of sample collection.

Nutrient and chlorophyll analyses

Water from each depth sampled was filtered through pre-combusted Whatman GF/F filters (0.7 µm nominal pore size) for measurements of particulate carbon (PC) and carbon stable isotope ratio ($\delta^{13}C$, as baseline for photosynthesis experiments), particulate phosphorus (PP), and chlorophyll *a*. PP measurements were made following the method of Stainton et al., (1977). PC and $\delta^{13}C$ were measured on an elemental analyzer (Costech Instruments ECS 4010 CHNSO Analyzer) coupled with an isotope ratio mass spectrometer (IRMS; Thermo Scientific DELTA V IRMS) using acetanilide as a standard.

In 2016, chlorophyll *a* measurements for whole-lake cruises were made following EPA SOP LG 404 (U.S.EPA, 2013). For collection depths not sampled by the EPA, chlorophyll *a* concentration was estimated from the CTD fluorescence profiles, based on the relationship between CTD fluorescence and extracted chlorophyll *a.* In addition to the EPA sampling in 2017, chlorophyll *a* was measured using a modified protocol. After filtration, chlorophyll *a* filters were stored in the dark at -10°C until analysis 2 to 7 days later. Filters were ground in a glass tissue grinder with 5 mL of extraction solution (68% methanol, 27% acetone, 5% DI water), after which the ground filter and solution were transferred to a test tube and another 5 mL of extraction solution was added, followed by extraction in the dark at -10°C for 24 hours. Following extraction, tubes were centrifuged, and fluorescence of the supernatant was measured with a Turner Designs 10-000 R fluorometer that had been calibrated following the procedure

described by Stainton et al., (1977). During the summer 2017 whole-lake survey, chlorophyll *a* concentrations measured with this method were higher than concentrations of matching samples measured with the standard EPA method. To facilitate comparison of all dates and locations, all chlorophyll *a* measurements made with the EPA method were adjusted using the equation Chlorophyll *a* = 1.28 (EPA chlorophyll *a*) + 0.03, $r^2 = 0.9855$).

Derivation of chlorophyll concentrations from fluorescence measurements

CTD chlorophyll *a* fluorescence profiles were converted to chlorophyll *a* concentration profiles by first correcting in situ fluorescence for quenching (decrease in fluorescence yield at high light intensities due to photo-protective processes). Several different approaches for correcting quenching have been used in the Great Lakes (Scofield et al., 2017; Bennion et al, 2019; Scofield et al., 2020). These corrections generally were derived by comparing extracted chlorophyll concentrations with fluorescence measurements made at different levels of PAR. We based our quenching correction on the relationship between the continuously monitored surface fluorescence and surface PAR values obtained during each survey. We found that the relationship between the fluorescence and PAR was well described ($r^2 > 0.65$) by a second-order polynomial or, in a simplified exponential form, as

$$F_c = F_m * \exp^{\gamma * PAR} \quad (1)$$

in which F_m is the measured fluorescence, F_c is the quenching-corrected fluorescence, γ is a survey-specific correction factor, and PAR has units μmol photons m^{-2} s^{-1}. We determined the values of the correction factors by linear regression after log-transforming Eq. 1. The correction factor values (γ) obtained were 0.000905 for spring 2016 ($log(F_m)$ = 1.01) and 0.000679 for summer 2017 ($log(F_m)$ = -0.036). Although this approach does not account for spatial differences

in near-surface fluorescence that are due to factors other than quenching, because the data span several day-night transitions we assume that any noise introduced into the relationship by spatial differences will have a negligible effect on the parameterization of the fitted equation.

After correcting for quenching, chlorophyll *a* fluorescence was converted to chlorophyll *a* concentration using the relationship between extracted chlorophyll *a* and CTD-measured fluorescence from nighttime CTD profiles or daytime CTD profile data from depths greater than 20 m, where quenching was negligible. Separate equations were developed for the spring 2016 whole-lake survey (Chl. $a = 1.19 * F_c - 0.1$; $r^2 = 0.77$), summer 2017 whole-lake survey (Chl. $a = 2.16 * F_c - 0.1$; $r^2 = 0.93$), and the 2017 seasonal sampling near Milwaukee (Chl. $a = 0.70 * F_c - 0.3$; $r^2 = 0.93$).

Photosynthesis experiments

The relationship between phytoplankton photosynthesis and irradiance was measured by using a benchtop incubator employing ^{13}C as a tracer (Hama et al., 1983). Controlled incubation provides highly reproducible results (Babin et al., 1994) and has been widely used since the method first was applied in Lake Michigan (Fee, 1973a). ^{13}C serves the same purpose as does ^{14}C in incubation experiments (Slawyk et al., 1977; Lee and Whitlege, 2005; Grosse et al., 2015), namely measuring the photosynthetic incorporation of inorganic carbon into the particulate organic fraction, but has the advantage of avoiding hazards associated with use of a radioisotope (Regaudie-de-Gioux, et al., 2014). Like the ^{14}C tracer method, measurements of production based on ^{13}C are thought to reflect something between net primary production (NPP) and gross primary production (GPP) (Marra, 2009; Milligan, et al., 2015), depending in part on the length of incubation time. Insofar as prior primary production measurements in Lake Michigan

(Fahnenstiel et al., 1989; Fahnenstiel and Carrick, 1988; Fahnenstiel and Scavia, 1987a; Fahnenstiel et al., 2010) have been made with the functionally equivalent ^{14}C incubation method, our ^{13}C measurements should be directly comparable (Hama et al., 1983; Regaudie-de-Gioux, 2014; López-Sandoval et al., 2018).

For each depth sampled, 5 L of unfiltered lake water was spiked with 80-90 mg of ^{13}C-labeled sodium bicarbonate ($NaH^{13}CO_3$, measured to 0.1 mg) to produce 9-10% inorganic carbon enrichment with ^{13}C. Spiked water was separated into 7 transparent 600 mL polycarbonate bottles and one dark bottle covered in aluminum foil. The incubator was illuminated by a 128-element LED light panel (Solla, Model SMD, 6500K) positioned at one end of the box. Bottles were incubated for 4 hours under a light gradient (0 to 1000 µmol photons m^{-2} s^{-1}) produced by a succession of neutral density filters placed between test chambers in the incubator. Light at each bottle position was measured using a spherical quantum scalar radiometer (Biospherical Instruments QSL-2101). Incubations were kept within 2 degrees of *in situ* temperature by adding ice to the incubator as needed and bottles were gently inverted every 30-60 minutes to minimize phytoplankton settling. After incubation, bottle contents were filtered through pre-combusted 25 mm diameter glass fiber (GF/F) filters, which were then rinsed several times with distilled, deionized water (DI) to remove any ^{13}C-labelled dissolved inorganic carbon (DIC).

DIC for each depth was calculated from measured pH assuming a constant carbonate alkalinity of 2148 µeq L^{-1} (Cai and Reavie, 2018). For sites near Milwaukee, pH was measured with the CTD. For whole-lake survey sites, pH was measured by the EPA according to EPA SOP LG 500 (U.S. EPA, 2019). The range of the 64 calculated DIC values was 2038-2199 µeq L^{-1} (median = 2137 µeq L^{-1}; mean = 2133 µeq L^{-1}). Mean offshore epilimnetic DIC based on direct gas chromatography measurements made in 2016 and 2017 was 2138.3 ± 39.6 µmol L^{-1}. At the

levels of ^{13}C enrichment used in our experiments, the range of calculated DIC values results in a potential error in photosynthetic rates due to uncertainty in DIC of ±4.1%.

The ^{13}C:^{12}C ratio of particulate organic carbon for each incubated sample and ambient background sample was measured on an IRMS, as described above. Photosynthetic rate was calculated as

$$P = \frac{C(a_{is} - a_{ns})}{t(a_{ic} - a_{ns})} \bullet 1.025 \quad (2)$$

where P = photosynthetic rate (mg m^{-3} hr^{-1}), C = POC concentration of the incubated sample (mg m^{-3}), a_{ns} and a_{is} are the ^{13}C atom % of POC at the beginning and end of the incubation, respectively, a_{ic} is the ^{13}C atom % of DIC after the ^{13}C spike, t is time (hr), and 1.025 corrects for isotopic discrimination (Hama et al., 1983). Dark bottle results were subtracted from each light bottle to account for anaplerotic CO_2 fixation (Williams and Lefèvre, 2008).

Size fractionation

To determine the degree to which different size classes of phytoplankton contribute to carbon fixation, particulate nutrient and photosynthesis samples collected at station AW75 from the chlorophyll *a* fluorescence maximum depth were separated into picoplankton (0.7-2 µm), nanoplankton (2-20 µm), and microplankton (20-200 µm) size classes on three occasions in 2017. Samples were passed through a 200 µm mesh to remove larger zooplankton, after which the filtrate was passed through a 20 µm mesh. Phytoplankton captured on the 20 µm mesh were backflushed with DI water and filtered onto a 0.7 µm GF/F filter to collect microplankton. The filtrate from the 20 µm mesh was filtered onto a 2 µm polycarbonate membrane filter, backflushed, and filtered onto a 0.7 µm GF/F to collect nanoplankton. Filtrate from the 2 µm membrane was filtered onto a 0.7 µm GF/F to collect the picoplankton.

Photosynthesis-irradiance (P-I) relationship

Photosynthetic rates normalized to chlorophyll *a* were fit to the three parameter photosynthesis-irradiance (*P-I*) model of Platt et al., (1980) using the 'fitPGH' function from the 'phytotools' package (Silsbe and Malkin, 2015) in R version 3.4.4 (R Core Team, 2018). This model is written

$$P^B = P_M^B \cdot \left(1 - e^{-\propto I/P_S^B}\right) \cdot e^{-\beta I/P_S^B} \quad (3)$$

where P^B is the photosynthesis rate normalized to biomass (mg C mg chl^{-1} hr^{-1}), P_M^B is the maximum photosynthesis rate (same units as P^B), P_S^B is a scaling parameter (same units as P^B), α^B is the initial slope of the P-I curve (mg C mg chl^{-1} mol photons^{-1} m^{-2}), I is irradiance (mol photons m^{-2} hr^{-1}), and β^B is the negative slope of the *P-I* curve when there is photoinhibition at high irradiance (same units as α^B).

When the photoinhibition parameter (β^B) was insignificant (95% confidence interval for β^B model fitting included zero; Fahnenstiel et al., 1989), the data were fit to the two-parameter model of Webb et al., (1974) using the 'fitWebb' function:

$$P^B = P_M^B \cdot \left(1 - e^{-\propto I/P_S^B}\right) \quad (4)$$

On four occasions, the photoinhibition parameter was statistically insignificant but photoinhibition was evident in the P-I curve, and the three parameter P-I model was used. PORT model optimization routines (Gay, 1990) were used for model fitting because they consistently provided the best fit to the data (lowest root mean square error). In one case for which the model fitting error was high (Spring 2016, MI17 2-m sample), P_M^B and α^B were determined manually.

P-I parameters from size fractionated incubations were normalized to chlorophyll *a* in each size class.

Areal production calculations

Areal production was calculated using the approach of Fee (1973a). For each day of sampling, k_{PAR} was calculated as the negative slope of natural log-transformed PAR versus depth, excluding irradiance from the upper 2 meters. The euphotic depth (0.5% of surface irradiance; Fee, 1990) was calculated as $5.3/k_{PAR}$. When the slope of the log (PAR)-depth relationship was not constant, indicating that k_{PAR} varied throughout the water column, two k_{PAR} values were applied. This typically occurred when the DCL was above the euphotic depth and the deeper k_{PAR} value was greater than the shallower value. For the few stations sampled at night (total of 6) or without an underwater PAR sensor (total of 4), k_{PAR} was estimated from its relationship with Secchi depth or CTD beam attenuation (Bukata et al., 1988) using functions determined from the daytime data from all cruises and beam attenuation measurements made between depths of 10 and 20 m. The resulting relationships were:

$k_{PAR} = 0.21$ [beam attenuation] + 0.08, $r^2 = 0.36$, (p-value = 0.0064) (5)

and

$k_{PAR} = 0.55$ [Secchi depth^{-1}] + 0.07, $r^2 = 0.42$, (p-value = 0.0049) (6)

Because our primary interest when examining the whole-lake survey data was in the spatial and temporal variations in photosynthetic capacity, rather than calculate the in situ photosynthetic rate at the time of sampling, we used long-term average values of cloud cover and atmospheric turbidity to scale calculated clear-sky irradiance estimates at each location. We also used this method for the study of the nearshore-offshore transects and when simulating annual

production at the time-series site. Clear-sky surface PAR (accounting for reflectance) was simulated at 30-minute intervals by using the 'incident' function from the 'phytotools' package (Silsbe and Malkin, 2015). Cloud-free atmospheric turbidity factors, which quantify the attenuation of solar radiation due to gaseous water vapor and aerosols in the atmosphere, were entered for each month and site to account for the seasonal and spatial variability of atmospheric turbidity (http://www.soda-is.com). On average between May and October 2017, cloud cover reduced daily surface irradiance measured on a buoy near Milwaukee by 26.5%. Therefore, all simulated PAR was multiplied by a constant 0.735.

For our experiment intended to evaluate the mechanisms controlling seasonal variation of production, we used the measured surface irradiance to calculate daily depth-integrated photosynthesis. From May to October 2017, shortwave radiation (W m^{-2}) was measured at 30-minute intervals on a 20 m buoy near Milwaukee. For November 2017, shortwave radiation data were obtained from the National Weather Service station in Horicon, Wisconsin (43.571 ºN, -88.609 ºW; https://mesowest.utah.edu/). Shortwave radiation was converted to PAR energy flux (W m^{-2}) assuming PAR energy is 46% of total shortwave radiation energy (Malkin et al., 2008). PAR energy flux was converted to photon flux (µmol photons m^{-2} s^{-1}) using a conversion factor of 4.6 µmol photons s^{-1} W^{-1} (Wetzel 2001). Irradiance at depth (I_z) was calculated as:

$$I_z = (1 - r) \bullet I_s \bullet e^{-k_{PAR} * z} \quad (7)$$

Where r is surface reflectance (a function of solar zenith angle), I_s is surface PAR measured in air, and z is depth.

All of our daily areal production calculations were performed using a modified version of the 'phytoprod' function in the R 'phytotools' package to allow for two depth-specific k_{PAR} values and two sets of P-I parameters (Fee, 1973b; Silsbe and Malkin, 2015). Photosynthesis was

calculated for every 0.1 m vertical interval and 30 min time interval, and then integrated over depth and time for each day. Daily production estimates for days not sampled were obtained by linearly interpolating the measured *P-I* parameters, k_{PAR}, and chlorophyll *a* concentration between dates (Fee, 1990).

We used the time-series observations made at station AW75 to assess the relative importance of the four variable categories (chlorophyll *a* concentration, surface irradiance, water clarity (k_{PAR}), and P-I parameters) that contribute to the modeled phytoplankton production by recalculating the daily production estimates holding three of the components constant and using the observed values for the fourth. We then quantified the relative contribution of each of the components to temporal variability as the percent departure from the mean daily production using only those days on which all four components were measured.

Finally, an index of phytoplankton growth rate (day^{-1}) was defined as the production (C fixation) to biomass (phytoplankton C) ratio (P:B). Phytoplankton carbon was calculated as 40% of total seston carbon. While the percentage of seston C that is living phytoplankton varies widely across lakes, it rarely exceeds 40% (Hessen et al., 2003). Therefore, our use of a value of 40% likely results in conservative estimates of the P:B ratio.

Possible Sources of Uncertainty

In addition to the uncertainty associated with our calculation of DIC noted above, other potential sources of error in our measurements are: 1) uncertainty in the values of the fitted P-I parameters including errors in the model fitting for individual incubations, 2) errors resulting from the assumption that we can apply the P-I parameters determined for a sample collected from a specific depth to a range of depths, and 3) errors due to the assumption of linear changes

in chlorophyll, water clarity, and P-I parameters between dates for the seasonal calculations. Following the example set by Fahnenstiel et al., (1989) we report the model fitting error (r^2) for each of our incubations in Tables 2-6. While the incubator simulated the depth gradient of total PAR within the lake, we did not attempt to simulate depth-related changes in the spectral quality of light within the lake, which may have resulted in underestimates of α^B for deeper parts of the euphotic zone (Larsson et al., 2021) and therefore modest underestimates of areal production. Linear interpolation between sampling dates is commonly used. Its accuracy depends on the frequency of sampling, and bi-weekly sampling appears to be adequate to capture major temporal trends (Fahnenstiel et al., 2010).

Results

Whole-lake surveys. We observed very little north-south variation in the primary variables (temperature, chlorophyll-a, and irradiance) during the spring (Fig. 2, Table 2). Values of spring surface water temperature (Fig. 2a) were similar (range 3.2 – 3.5 °C) across all sites except at MI-N, where it was 2.2 °C. Spring chlorophyll *a* concentration (Fig. 2b) also was similar across sites, with a range of 0.44 – 0.79 mg m^{-3}. Mean percent surface irradiance (Fig. 2c), determined as the mixed layer average PAR to surface PAR ratio (Fahnenstiel et al, 2000), was highest at the northern-most station due to its bottom depth being shallower than the euphotic zone depth (Table 1).

There was more north-south variability in these variables during the summer. Temperatures were warmer in the south, but chlorophyll was higher in the northern areas, which resulted in a south to north decrease in mean percent surface irradiance in the mixed layer. The mixed layer depths were similar across stations (13 – 19 m), but the water clarity was lower in

the northern basin. Mean k_{PAR} was 0.112 m^{-1} in the southern basin and 0.148 m^{-1} in the northern basin.

Areal production (Fig. 2d) in spring was highest at MI23 (337 mg C m^{-2} day^{-1}) and lowest at MI17 (201 mg C m^{-2} day^{-1}) and within in a narrow range (243 – 253 mg C m^{-2} day^{-1}) at the other stations. Compared to the spring survey, areal production was higher in the summer throughout the lake and generally increased from south to north where chlorophyll concentration also was higher. Areal production ranged from 316 mg C m^{-2} day^{-1} at the southern-most station MI11 to 549 mg C m^{-2} day^{-1} at the northern-most station MI52.

Spring P:B ratios, interpreted as a proxy for phytoplankton growth rate, were similar across sites (Fig. 2e) except for the southernmost site (MI17) where it was approximately 75% of the mean value for the other sites (seston carbon was not measured at station MI47). Summer P:B ratios in the southern area of the lake (Stations MI11 and MI23) were similar to the spring values but increased toward the north where production was highest.

The seston carbon to phosphorus (C:P) ratio (Figure 2f) tended to be higher during the summer than during the spring and showed a slightly decreasing south to north trend. Using the criterion established by Healy and Hendzel (1980), the C:P ratios suggest moderate phosphorus deficiency ($128 < C:P < 258$) at all stations except MI23 (south) and MI34 (central lake) where the deficiency was severe (C:P ratios of 274 and 275 respectively).

Estimates of surface chlorophyll concentration obtained from satellite imagery (Lesht et al., 2013; 2016) and measurements from the continuous flow fluorometer operated while underway (Fig. 3) show that during the spring much of the lake was horizontally homogeneous, consistent with the grab sample data. During the summer the northern stations with higher chlorophyll values were closer to shore where the satellite imagery also shows higher values.

Overall, the model (Eqs. 3 and 4) fits to the photosynthesis data were very good. For the 64 experiments conducted in 2016 and 2017 (Table 1) the median r^2 value was 0.9640, the mean was 0.9130, and the first and third quartiles were 0.8885 and 0.9838. During the spring, only two of the photosynthesis experiments (Table 2) exhibited photoinhibition. These two were the mid-depth samples at the southern basin stations (MI17 and MI23). Values of P_M^B in the surface water increased from south to north in the spring (Figure 4a), ranging from 0.88 (mg C mg Chl^{-1} hr^{-1}) at MI17 to 1.41 at MI-N. Except for MI17, the values of α^B (Figure 4c) in the surface samples were fairly consistent (range 8.03 to 11.8 mg C mg Chl^{-1} mol $photons^{-1}$ m^2, mean = 9.6 ± 1.6); the estimated α^B value at MI17 was lower (3.07 mg C mg Chl^{-1} mol $photons^{-1}$ m^2). We found no relationship between either the spring P_M^B or α^B values and temperature or chlorophyll *a* concentration.

In contrast to the spring, all except one (MI23, 5m sample) of the summer 2017 photosynthesis experiments showed photoinhibition (Table 3). Though the sub-thermocline P_M^B values north of Green Bay were higher than at the other stations (Figure 4b), there was no significant difference (Kruskal-Wallis test) between the means of spring and summer values of surface P_M^B at the main lake stations (excluding DC75 and GB1). The mean P_M^B value of the summer sub-thermocline fluorescence maximum samples was 42% lower than that of the epilimnion samples, but they were only significantly different at the 0.075 level (H=3.17, p = 0.075).

Overall, the modeled values of α^B (Figure 4d) were significantly (H=6.86, p=0.009) higher in the combined mid-depth and sub-thermocline samples than in the epilimnion samples (respective mean values of 7.84 and 5.72) and significantly (H=7.01, p=0.008) higher in the

spring (mean = 8.98) than in the summer (mean = 4.59). There was no discernable north-south pattern to the α^B values in either the spring or summer surveys at either depth level.

As noted above, all but one of the summer survey samples showed evidence of photoinhibition, as indicated by non-zero values of β^B. We found no significant difference in the values of β^B when we compared the epilimnion samples (mean = 0.17 ± 0.09) with the sub-thermocline samples (mean = 0.27 ± 0.13).

Seasonal production. At AW75, daily areal production generally increased from May to August and decreased from August to November (Figure 5a). Over the period of measurements (May – November), mean monthly production (± 1 standard deviation) was highest in August (585 ± 107 mg C m^{-2} day^{-1}) and lowest in May (287 ± 61 mg C m^{-2} day^{-1}; Figure 5b). Mean summer production (when surface temperature was >15°C) was 499 ± 129 mg C m^{-2} day^{-1}. To estimate annual production at AW75, mean production for the months of December - April was assumed to be 200 mg C m^{-2} day^{-1} (Figure 2c in Fahnenstiel et al., 2010), which results in a total annual production of 120 g C m^{-2} $year^{-1}$.

Based on our sensitivity analysis, variation in the P-I parameters had the greatest influence on temporal variance of total areal production, followed by chlorophyll *a*, surface irradiance, and water clarity (Figures 5c-d). The proportions of temporal variance in areal production attributable to water clarity (k_{PAR}), surface irradiance, chlorophyll *a*, and P-I parameters during the study period were 16.0%, 18.8%, 24.7%, and 39.7%, respectively. During the spring when areal production was low (Figure 5a), surface irradiance and water clarity were favorable for production (Figure 5d), but their effect was offset by low chlorophyll *a* concentrations and photosynthetic efficiency (i.e., low values of P_M^B and α^B; Figure 5c). As

temperatures warmed from May to August, epilimnetic chlorophyll *a* concentration, P:B, P_M^B, and C:P increased (Figure 6). By the time of peak areal production in late August, declining water clarity and surface irradiance had a slight negative effect on areal production (Figure 5d), but these effects were small relative to the positive influence of high photosynthetic efficiency (i.e., high P_M^B) and chlorophyll *a* concentration (Figures 5c, 6e).

Epilimnetic and mid-depth phytoplankton displayed different photosynthetic characteristics (Table 4, Figure 6e and f). P_M^B was higher in the epilimnion during the stratified period and increased from May to August following the increase in temperature. The highest epilimnetic P_M^B values were measured on August 29 and October 9, corresponding to some of the lowest C:P ratios and the highest growth rates during the stratified period. Mid-depth P_M^B decreased from May to late June as the DCL formed, then increased as the DCL broke down. Low P_M^B in the DCL corresponded to high C:P ratios, low phytoplankton C:Chl, and low P:B ratios. The highest mid-depth P_M^B occurred in October at the base of the epilimnion and in the metalimnetic oxygen maxima. Mean epilimnetic and mid-depth P_M^B from May to October were 1.73 and 1.12 mg C mg chl^{-1} hr^{-1}, respectively.

Photosynthetic efficiency at suboptimal PAR values, as reflected in α^B (Figure 6f), was generally lower in epilimnetic phytoplankton. Mean ± 1σ of epilimnetic and mid-depth α^B from May to October were 6.75 ± 3.26 and 9.65 ± 5.23 mg C mg chl^{-1} mol photons^{-1} m^2, respectively. Epilimnetic α^B decreased, as did the seston C:P ratio in July and August. Mid-depth α^B was variable throughout the season but showed a generally increasing trend from spring to fall. Within the DCL, α^B increased as the DCL grew and moved deeper into the water column. The epilimnetic light saturation parameter (I_k), defined as P_M^B / α^B (Fahnenstiel et al., 1989), generally increased from May to August (Table 4) following the increase in temperature and C:P, then

decreased in late August and September when nutrient limitation decreased. I_k was lower in mid-depth phytoplankton than in epilimnetic phytoplankton and decreased within the DCL over time, suggesting greater low-light acclimation in the deeper communities.

Following the onset of stratification in June (Figure 7a), a DCL developed in the hypolimnion (Figure 7b). 71-74% of total water column production occurred below the relatively shallow epilimnion during the early DCL period in June, and 18-23% of total water column production occurred within the DCL (Figure 7c). As the DCL deepened in the water column in July, DCL C:P and photo-acclimation (as reflected in C:Chl and α^B) increased, DCL P:B ratios declined, and DCL production decreased to only 6% of total water column production (Figure 8). DCL production averaged 15% of total water column production when a DCL was present, and epilimnetic production during the stratified period averaged 62% of total water column production.

From August to November 2017, temperature, irradiance, areal production, and epilimnetic P:B declined. In October, P_M^B and α^B were high, but production declined due to decreased irradiance and chlorophyll *a* concentration (Figure 5). Peaks in volumetric production were observed at the base of the epilimnion (10 m) and metalimnetic oxygen maxima (16 m) when these depths were sampled in October (Figure 7c). In November, epilimnetic chlorophyll concentration increased following the breakdown of stratification (Figures 6a, 7b), but production declined further due to low irradiance and P_M^B and α^B values (Figures 6e-f).

Nearshore-offshore transects. During July, the water column was more strongly stratified offshore than nearshore (Figure 9a); strength of stratification was assessed by the temperature difference across the thermocline. The thermocline depth increased by 8 m from station AW45 to

station AW75 and the surface water temperature increased from 10.5 °C at station AW15 to 15.7 °C at AW45 to 18.4 °C at AW75, suggestive of moderate nearshore upwelling. At this time epilimnetic chlorophyll *a* concentration was highest nearshore at AW15 (4.01 mg m^{-3}) and decreased with distance offshore to 0.91 mg m^{-3} at AW75 (Figure 9b, Table 5). A DCL was present at a depth of ~25 m at the AW45 station and ~35 m at the AW75 station (Figure 8a). Both P_M^B and α^B decreased from nearshore to offshore which, along with the higher nearshore chlorophyll *a* concentrations, resulted in higher epilimnetic production closer to shore (Fig 9c). Although photoinhibition was not observed in the July epilimnion samples, the sub-thermocline photosynthesis measurements were best fit with the three-parameter model and the values of P_M^B, α^B, and β^B were not significantly different between AW45 and AW75.

At the height of stratification in September the thermocline had deepened and the surface water temperature had increased to over 18° C at all three stations (Figure 10a). Epilimnetic chlorophyll *a* concentrations (Figure 10b) were lower at AW15 and AW45 than in July but higher offshore at AW75 (1.60 mg m^{-3} compared to 0.91 mg m^{-3}). Surface P-I parameters were highest at AW15. Sub-thermocline α^B values at AW45 and AW75 were significantly higher than in the epilimnion, and phytoplankton collected from these depths exhibited photoinhibition when exposed to high irradiance. Areal production was still highest nearshore, though offshore production in September was approximately double what it was in July. Epilimnion seston C:P was lowest nearshore (C:P = 116 at AW15) and increased offshore to approximately 193 at both AW45 and AW75.

In October, after the lake began to cool, the temperature (Figure 11a) at the surface was higher offshore (14.8 ºC at AW75) than nearshore (7.1 ºC at AW15). Compared to September, chlorophyll concentrations in the epilimnion decreased at stations AW15 and AW75 but was

unchanged at AW45. Sub-epilimnion chlorophyll values were higher at all stations than in the epilimnion. No photoinhibition was found in the epilimnion samples. Most of the production in October had shifted offshore where both the chlorophyll *a* concentration and P:B ratios were highest (Figures 11b-c). Seston C:P was lowest nearshore (C:P = 95 at AW15) and increased with distance offshore (C:P = 150 at AW45, and 215 at AW75).

Size fractionation. There was a slight loss of chlorophyll *a* through the size fractionation procedure in June and July (sum of size classes 22% lower than bulk seston chlorophyll *a* concentration). In September, it appeared that nanoplankton chlorophyll *a* was undermeasured (7% of total chlorophyll *a*), as the proportion of measured nanoplankton particulate carbon was 22%, similar to the nanoplankton fraction of chlorophyll *a* observed by Carrick et al., (2015). Therefore, nanoplankton chlorophyll *a* was instead calculated as the difference between bulk chlorophyll *a* and the sum of microplankton (46% of total) and picoplankton chlorophyll *a* (36% of total), resulting in 18% nanoplankton chlorophyll *a*.

In mid-depth size-fractionated experiments, picoplankton (< 2 µm) was consistently the dominant fraction of total chlorophyll *a* (> 46%) and the contributions of nanoplankton (2-20 µm; 18-29%) and microplankton (20-200 µm; 18-36%) were roughly equal (Table 6). When the DCL was present in June and July, picoplankton displayed the highest P_M^B, along with high α^B and low I_k values, suggestive of low light acclimation. In September when a DCL was not present, P-I parameters were variable and there was no consistent pattern among size classes (Table 6).

Discussion

Spatial patterns. Spatial patterns of phytoplankton production in Lake Michigan varied depending on the season. During the spring isothermal mixing period temperature, areal production, chlorophyll *a* concentrations, and growth rates (as indicated by P:B), were similar across offshore sites, with no evident south-north spatial pattern (Fig 2). The lack of spatial pattern in offshore spring production, chlorophyll *a*, and P:B may have been due to homogeneous physical and chemical conditions during spring isothermal mixing when temperatures are low, and nutrients are mixed throughout the water column. Satellite imagery (Fig 3a) also shows that spring chlorophyll concentration across the lake was nearly uniform except in limited coastal areas we did not sample.

Spring isothermal mixing in Lake Michigan has been characterized by suboptimal nutrient, light, and temperature conditions for phytoplankton growth, with previously reported growth rates being < 0.19 day^{-1} (Fahnenstiel et al., 2000). However, our offshore spring isothermal P:B ratios averaged 0.34 day^{-1}. This is similar to Fahnenstiel et al.'s (2000) measurements of what spring growth rate could be if light- and nutrient-limitation are alleviated (0.3 day^{-1}). The higher spring growth rates measured in this study may be due to increased water clarity (Binding et al., 2015; Yousef et al., 2017), increased nutrient supply due to recycling by dreissenid mussels (Shen et al., 2018), the increased dominance of picoplankton (Kagami and Urabe, 2001), or some combination of these three factors. Seston C:P ratios (Fig. 2f), an indicator of phytoplankton nutrient status, suggest phosphorus deficiency was absent or moderate at all offshore sites except for MI17 in the spring. Furthermore, mean irradiance in the 2016 spring mixed layer was 12% of surface irradiance, compared to 4% observed by Fahnenstiel et al. (2000) in 1993-1995. If spring phytoplankton growth rates have indeed increased since the mussel invasion, this suggests that the post-dreissenid reductions in spring phytoplankton

biomass and areal production are the result of an increase in some phytoplankton loss pathway, with dreissenid mussel grazing seeming the most likely. We note, however, that the method used by Fahnenstiel et al. (2000) to determine phytoplankton growth rate (^{14}C labeling into chlorophyll) is different from our approach, and a more conclusive comparison of growth rates over time will require additional measurements using similar methods.

Satellite imagery showed that a sediment resuspension ("plume") event occurred in the region of the MI17 site prior to the day of sampling in spring 2016 (NASA/GSFC, 2018: MODIS image A2016086184500), which may explain both the high C:P ratio and the low P:B ratio at this station. Although sediment resuspension events may be a source of limiting nutrients and can increase phytoplankton growth (Millie et al., 2003), they can also increase turbidity and decrease light availability, which can decrease depth-integrated phytoplankton production and in situ growth rates (Eadie et al., 1984; Eadie et al., 2002; Lohrenz et al., 2004). Water clarity at MI17, however, was not lower than at the offshore sites, suggesting the low P:B and high C:P may have been due to high non-algal carbon concentrations from resuspended sediment rather than reduced production or growth. The effects of sediment resuspension on phytoplankton productivity may depend on the time of sampling within the sediment resuspension event (Lohrenz et al., 2004).

During summer stratification, the northern basin of Lake Michigan exhibited lower phosphorus limitation (inferred from seston C:P), and higher production, P:B ratios (Fig. 2e), and chlorophyll *a* concentrations (Fig. 2b) than the southern basin. Remote sensing estimates of chlorophyll concentration (Fig. 3b) also suggest areas of high production in the northern basin, specifically off the coast of Door County and near the mouth of Green Bay (U.S. EPA. 2021), implying localized nutrient input. Higher northern basin productivity may be due to higher TP

concentrations in the north (Cai and Reavie, 2018), perhaps due to nutrient input from eutrophic Green Bay. Although the main northern basin of Lake Michigan directly receives only ~15% of the total phosphorus load to Lake Michigan, Green Bay receives 30% of the lake's total P load (Dolan and Chapra, 2012). A significant portion of the load to Green Bay is lost to sediment burial within the bay (Klump et al., 1997), but the relatively small cross-sectional area connecting Green Bay to the lake proper likely results in a significant localized effect on nutrient concentration and phytoplankton production in the open lake, depending on the path and mixing rate of water after it leaves Green Bay.

While Fahnenstiel et al., (2016) also observed higher chlorophyll *a* concentrations in the northern basin, they found no significant difference in daily areal production between the northern and southern basins of the lake when averaged across all depth zones. The differences between their findings and ours may be due to methodological differences (remote sensing of nearshore to offshore vs. one whole-lake summer survey at mostly offshore sites) or meteorological or nutrient loading differences among years. If phytoplankton productivity is indeed higher in the northern basin, this may result in greater productivity at higher trophic levels in the north. Satellite-derived surface chlorophyll *a* concentrations have been shown to correlate to fish yield in other aquatic systems (Ware and Thomson, 2005), and the relatively phosphorus-rich phytoplankton (suggested by low seston C:P) may result in more efficient trophic transfer (Sterner et al., 1997; Sterner and Hessen, 1994).

Seasonal patterns. Prior to the mussel invasion, phytoplankton production typically peaked during late spring due to the upward mixing of nutrients and reduction in light limitation, stimulating a spring diatom bloom (Fahnenstiel et al., 2010). Mussel grazing has significantly reduced the size of the spring diatom bloom and has reduced spring and early summer

production by 78% and 22%, respectively (Fahnenstiel et al., 2010). In 2017, phytoplankton production at AW75 peaked in August and September during the period of warmest temperatures, similar to trends observed in 2007 and 2008 (Fahnenstiel et al., 2010). However, production during this peak period (499 mg C m^{-2} day^{-1}) was less than that measured in the 1980s, before dreissenid mussels were established in the lake (867 mg C m^{-2} day^{-1}; Table 4 in Fahnenstiel et al., 2010).

Overall, the factors controlling areal production varied among seasons. During the spring, high surface irradiance and water clarity should provide favorable conditions for production, but spring production was low due to low chlorophyll *a* concentrations which were likely the result of heavy mussel grazing (Rowe et al., 2015; Fahnenstiel et al., 2010) and low spring temperatures (Geider and Osborne, 1992, Fahnenstiel et al., 2000). P-I parameters also were low in the spring. Chlorophyll *a* -normalized P-I parameters are responsive to environmental conditions and can be indicators of phytoplankton physiological status. α^B characterizes the photochemical reactions of photosynthesis and is dependent on light history and availability, nutrient availability, and taxonomic composition (Edwards et al., 2015; Platt and Jassby, 1976; Talling, 1957; Welschmeyer and Lorenzen, 1981). P_M^B is a function of the enzymatic reactions of photosynthesis and is dependent on temperature, nutrient availability, light history, and taxonomic composition (Fahnenstiel et al., 1989; Geider and Osborne, 1992; Harding et al., 1987; Senft, 1978; Talling, 1957). As stratification developed, epilimnetic chlorophyll *a* concentrations and P:B ratios increased, likely due to warming temperatures and restricted access of benthic mussels to the euphotic zone (Rowe et al., 2015). This accelerated growth likely depleted dissolved P concentrations in the eplimnion, leading to greater nutrient limitation as inferred from the increase in the seston C:P ratio.

As stratification strengthened in summer, a DCL developed below the thermocline (Fig. 7). The Lake Michigan DCL is highly dynamic and the mechanisms controlling the DCL varied throughout the season. When the DCL was shallowest in the water column during June, DCL P:B ratios (Fig. 6b) and DCL phytoplankton production were greatest, suggesting *in situ* growth is important for initial DCL formation (Fahnenstiel and Scavia, 1987b; Scofield et al., 2020). As the DCL moved deeper into the water column, phosphorus limitation (inferred from seston C:P) and low-light acclimation (inferred from α^B) increased, and P:B ratios and volumetric production decreased. Therefore, as the DCL deepens, it appears that maintenance of the DCL is due more to photo-acclimation (increased chlorophyll *a* per unit biomass; Geider 1987) than to *in situ* phytoplankton growth.

In phytoplankton communities that exhibit photoinhibition, low-light adaption is associated with lower levels of irradiance (I_{opt}) above which growth is inhibited (Edwards et al., 2015). We calculated I_{opt} by finding the value of irradiance that corresponded to the maximum value of P_M^B calculated from the P-I model (Eqs. 3,4). Figure 12 shows the relationship between I_{opt} and I_k, the light saturation parameter, also an indicator of photoacclimation, for samples collected at different depths. The relationship between the two is strongly linear, and lower values of both I_{opt} and I_k are found in the deeper, presumably more low light-adapted communities. This indicates that the photosynthesis-light response of Lake Michigan phytoplankton differs between depths due to light acclimation, especially after stratification, which further implies that algal photo-acclimation time scales are shorter than vertical mixing time scales.

No DCL was observed at the offshore site in southwestern Lake Michigan in August and September. Other studies have also reported a diminishing of the DCL in late summer, although

rarely a complete disappearance as was observed in this study (Fahnenstiel and Scavia, 1987b; Fahnenstiel et al., 2010; Pothoven and Fahnenstiel, 2013). We did not investigate zooplankton dynamics, Fahnenstiel and Scavia (1987b) found that high zooplankton abundance in the DCL in August increased the loss of phytoplankton to grazing and resulted in a relatively rapid decrease in phytoplankton abundance at depths of 20 to 40 m. In general, the apparent mechanisms controlling the DCL in this study appear to be consistent with past studies: *in situ* growth is most important early in the stratified season and photo-acclimation increases as the DCL moves deeper into the water column (Schofield et al., 2020). The zooplankton grazing observed by Fahnenstiel and Scavia (1987b) also may reduce the size of the DCL in late summer, but our work does not speak directly to that process.

In prior studies, DCL production during the June-July period averaged 36 ±18% of total water column production in Lake Michigan (range = 13-74%, n = 10; Fahnenstiel and Scavia 1987b). By comparison, our three June-July measurements of DCL production in 2017 accounted for an average of only 15±9% (range 6-23%, n = 3) of total water column production. Based on the Welch One-Way ANOVA test, this difference between the two is significant ($p=0.029$). Fahnenstiel and Scavia (1987a) also observed the presence of a deep DCL in August, whereas in 2017 the DCL had disappeared by late July (Fig. 7b). Recent increases in water clarity (Binding et al., 2015) might be expected to increase DCL production, but because the DCL is almost always below the thermocline, vertical mixing within the hypolimnion may give profundal mussels access to this resource (Shen et al., 2018), and mussel grazing may counter the effect of greater water clarity.

As production has declined in Lake Michigan, phytoplankton community composition has also shifted. Diatoms and other microplankton (> 20 µm) have decreased, while the relative

abundance of cyanobacteria and picoplankton has increased (Carrick et al., 2015; Reavie et al., 2014; Fahnenstiel et al., 2010). The greater decrease in diatoms and other microplankton is hypothesized to be the result of selective mussel filtering (Vanderploeg et al., 2001), as dreissenid mussels prefer to consume larger, nutritious diatoms and microzooplankton over less nutritious, smaller phytoplankton, such as cyanobacteria (Nalepa and Schloesser, 2013).

Our results are consistent with past studies illustrating a shift towards picoplankton dominance of the Lake Michigan phytoplankton community (Fahnenstiel et al., 2010; Engevold et al., 2015; Carrick et al., 2015). Picoplankton was the dominant fraction of total chlorophyll *a* in 2017 and displayed the highest P_M^B and α^B in the DCL community (Table 6). Higher P-I parameters in picoplankton may be due to smaller cells having greater mass-specific phosphorus uptake capacity than larger cells and greater light harvesting abilities due to less self-shading (Grover, 1989). Picoplankton dominance may have implications for energy transfer to higher trophic levels, as picoplankton may increase the number of trophic transfers between primary producers and fish (Carrick et al., 1991), and may be less nutritious than larger phytoplankton (Lampert, 1987).

Areal production peaked in late August, corresponding to the warmest temperatures, lowest nutrient limitation (C:P), highest P-I parameters, and greatest growth rates (P:B), suggesting both temperature and a temporary reduction in nutrient limitation supported high production. In Lake Superior, recent algae blooms have been linked to periods of exceptionally warm temperatures, and warming lake surface water temperatures with climate change may be affecting phytoplankton production in the Great Lakes in general (Reavie et al., 2017). A reduction in nutrient limitation during the period of warmest temperatures may be due to increased nutrient recycling at warmer temperatures (Scavia, 1979; Rigler, 1973). Although

many factors control epilimnetic nutrient recycling in the Great Lakes (Scavia, 1979), zooplankton-driven nutrient recycling has the greatest influence on offshore epilimnetic phosphorus dynamics during the summer (Scavia and Fahnenstiel, 1987; Scavia, 1979; Scavia et al., 1988). In 2017, nutrient limitation (as inferred from seston C:P) was lowest during the period when zooplankton abundance is usually greatest (Vanderploeg et al., 2012; Driscoll and Bootsma, 2015). However, while phytoplankton production was higher during late summer, if this is due to greater epilimnetic nutrient recycling then it may not indicate an increase in net ecosystem production, as phytoplankton production would reflect energy and nutrients being recycled within the epilimnion by producers and consumers rather than newly fixed carbon.

During the fall, production declined due to cooling temperatures and declining surface irradiance. P-I parameters peaked in October and chlorophyll *a* concentration increased with the breakdown of stratification and reduced epilimnetic nutrient limitation (seston C:P), but the effect of these increases on production was minimized by the inhibiting effects of declining surface irradiance and temperature, and in fact the increase in P-I parameters, along with low C:Chl ratios, likely reflect relief from strong nutrient limitation as the system shifts toward stronger light limitation.

In general, it appears that temperature and light availability have the strongest influence on seasonal patterns of production in Lake Michigan. Similar observations have been made for Lake Superior, where seasonal variation in production can be modeled well with only temperature and light data (Sterner, 2010). Likewise, Fahnenstiel et al., (2016) found temperature to be a good predictor of P_M^B in the upper Great Lakes, and P_M^B in turn has a strong influence on areal production. Although temporary reductions in nutrient limitation inferred from seston C:P ratios corresponded to high P:B ratios and P-I parameters in this study, the seasonal

trends in production and epilimnetic P:B were strongly related to the seasonal temperature trends. In the offshore zone of Lake Michigan, Lake Superior, and perhaps other oligotrophic Great Lakes, phytoplankton are consistently nutrient limited, and seasonal trends in production appear to be more strongly controlled by variation in temperature and light.

Nearshore-offshore patterns. Nearshore-offshore phytoplankton production gradients appear to be strongly influenced by upwelling. Remote sensing (www.greatlakesremotesensing.org) revealed strong upwelling along the western shore of Lake Michigan for several days prior to the day of July transect sampling, and re-stratification on the day of sampling. Production, P:B ratios, and chlorophyll *a* concentrations were highest nearshore (AW15), where temperatures were coolest, but the seston C:P ratio was lowest at the mid-depth site (AW45). In October, remote sensing also showed upwelling nearshore several days prior to and on the day of sampling, but in contrast to conditions in July, chlorophyll *a*, production, and P:B ratios generally increased from nearshore to offshore following the trend in temperature. Nutrient limitation, however, as inferred from seston C:P, was lowest nearshore and increased with distance offshore. Based on these sampling events, there appears to be no simple relationship between upwelling and productivity. Nearshore upwelling is highly variable in extent, magnitude, and duration (Plattner et al., 2006), and its effects on phytoplankton communities are varied (Haffner et al., 1984; Pilcher et al., 2015). Upwelling can bring growth-promoting nutrients to the nearshore euphotic zone, and if upwelling is from mid-depth regions it can transport phytoplankton-rich water from the DCL to the nearshore zone. However, strong upwelling can also inhibit nearshore production by lowering temperatures and replacing phytoplankton-rich water with phytoplankton-poor hypolimnetic water (Haffner et al., 1984). As a result, the effect of upwelling on phytoplankton productivity may be expected to vary with

each upwelling event depending on the depth of origin of upwelled water and the duration of upwelling.

In September, remote sensing revealed no evidence of upwelling or downwelling prior to the day of transect sampling. The lake was strongly stratified from nearshore to offshore, and production, chlorophyll *a* concentrations, and P:B ratios were highest nearshore where seston C:P ratios were lowest. Lower nearshore nutrient limitation and higher productivity may be due to multiple factors. Nearshore regions typically have elevated nutrient and chlorophyll *a* concentrations compared to offshore regions due to retention of river-borne nutrients in nearshore zone (Rao and Schwab, 2007; Stadig et al., 2020; Warren et al., 2017; Yurista et al., 2015). In addition, mussel excretion can represent a significant input of dissolved nutrients to the nearshore zone (Ozersky et al., 2009; Bootsma and Liao, 2014; Bravo et al., 2019). Although phytoplankton biomass can be lost to mussel grazing in the nearshore zone (Rowe et al., 2015; Yousef et al., 2014) the positive effects of mussel nutrient excretion on phytoplankton production may outweigh the negative effects of grazing in a relatively shallow water column where depth-averaged irradiance is high (Zhang et al., 2011). The influence of mussel nutrient excretion on phytoplankton growth rates has not been accounted for in many modeling studies, but it may be especially important to consider in the nearshore zone where mussels, phytoplankton and nutrients are more tightly coupled year-round (Waples et al. 2016).

Based on remote sensing data from 2010 to 2013, Fahnenstiel et al., (2016) found no differences in mean chlorophyll *a* concentration among shallow (0-30 m), mid-depth (30-90 m), and deep (> 90 m) depth zones in Lake Michigan. However, they did conclude that production in the shallow region was lower than in the mid-depth and deep regions. Phytoplankton production may be expected to differ along nearshore-offshore gradients, as nearshore variability is greater

due to the influence of external nutrient loading, upwelling, sediment resuspension, and complex nearshore currents (Eadie et al., 2002; Plattner et al., 2006; Yurista et al., 2015). Mussel densities also differ among depth zones and substratum (Nalepa et al., 2014). Lower production in the shallow region estimated by Fahnenstiel et al., (2016) may be attributable to limitations of remote sensing in shallow nearshore waters, occurrences of upwelling, filtering by mussels reducing the productive biomass, or a smaller volume of water per square meter over which production can occur. In Lake Superior where mussel densities are low, Fahnenstiel et al., (2016) found significantly higher chlorophyll *a* concentration, but lower production nearshore compared to offshore, suggesting that the lower nearshore production they observed in Lake Michigan may have been due to factors other than dreissenid grazing. As nearshore upwelling occurs somewhere in Lake Michigan during 59% of the stratified season (Plattner et al., 2006), and the effects of upwelling on phytoplankton are variable (Haffner et al., 1984; Pilcher et al., 2015), it is possible that upwelling may play a greater role than mussel grazing in controlling nearshore-offshore patterns in production. From a food web perspective, it is important to recognize that much of the primary production in the nearshore zone is in the form of benthic algae, which was not measured in this study, and this production may be an important source of energy for higher trophic levels (Turschak et al., 2014; Turschak and Bootsma 2015).

Comparison with previous studies. The results of this study support previous findings of decreased areal phytoplankton production and changes to the phytoplankton community since the quagga mussel invasion in Lake Michigan. Mean areal summer phytoplankton production in 2017 (499 mg C m^{-2} day^{-1}) was 42% lower than production reported by Fahnenstiel et al., (2010) prior to the mussel invasion (1983-87: 867 mg C m^{-2} day^{-1}) and 26% lower than the production they measured in 2007 and 2008 after the mussel invasion (677 mg C m^{-2} day^{-1}). Although the

differences between production measured in this study and the post-dreissenid measurements reported by Fahnenstiel et al., (2010) may be due in part to the increase in profundal quagga mussel densities over the past decade (Nalepa et al., 2014), the apparent declines since 2008 also may be due to differences between study locations (west vs east) and inter-annual variability related to factors such as meteorological conditions and planktivore abundance. We note that despite these differences in location the temporal patterns of production are very similar in both studies.

Our calendar summer (June – August) production estimate of 460 mg C m^{-2} day^{-1} at AW75 is similar to the mean 2010 to 2013 summer lake-wide production estimate of 499 mg C m^{-2} day^{-1} that Fahnenstiel et al., (2016) estimated based on satellite imagery. If water column production was indeed similar in both study periods, the error of remotely derived estimates of phytoplankton production due to vertical variability within the water column appears to be modest despite our finding that deeper phytoplankton are more photosynthetically efficient at low light than shallower ones. This study indicates that most production during stratification now occurs within the epilimnion and only 6-23% occurs within the DCL, suggesting remote sensing production estimates obtained using surface values may not severely underestimate production. Increased photosynthetic efficiency in the DCL appears to be offset by reduced DCL biomass compared to pre-mussel conditions.

Although phytoplankton production has significantly declined in Lake Michigan since the mussel invasion, spring P:B ratios, a proxy of phytoplankton growth rates, appear to have increased, which may be due to increases in water clarity (Binding et al., 2015), nutrient excretion by mussels (Shen et al., 2018) and an increase in the proportion of picoplankton (Kagami and Urabe, 2001). Summer P:B ratios, however, do not appear to have changed since

prior to the mussel invasion. Comparing our epilimnion data to those presented in Fahnenstiel and Scavia (1987b) using similar sampling dates (May-July), we find the mean 1982-1984 P:B of 0.312 ± 0.179 to be not significantly different from our mean P:B of 0.379 ± 0.095 ($p = 0.53$).

P-I parameters in 2017, however, differed from the pre-mussel period (Table 4). Mean epilimnetic α^B in 2017 was slightly higher than mean epilimnetic α^B from 1983 to 1987, and mean epilimnetic P_M^B in 2017 was nearly half of mean epilimnetic P_M^B during the 1980s. These P-I parameter comparisons, however, depend greatly on how the P-I parameters are summarized from each study, as averaging P-I parameters across different seasons and different years can produce dramatically different results (Fahnenstiel et al., 1989). These comparisons across decades are also complicated by interannual and spatial variability of P-I parameters and methodological differences among studies. As a result, historical comparisons of P-I parameters may not be the best indicator of changes to the phytoplankton community, and we suggest phytoplankton growth rates may be a better integrator of ecological conditions.

The lack of obvious changes in summer phytoplankton growth rates and the apparent increase in spring growth rates since the mussel invasion was somewhat unexpected. Declining offshore total phosphorus concentrations (Barbiero et al., 2018; Mida et al., 2010) might be expected to result in increased phosphorus limitation and decreased phytoplankton growth rates. However, phytoplankton do not direly rely on total phosphorus. They rely on dissolved phosphate, and the post-dreissenid decrease in total P may be more of a reflection of the decrease in phytoplankton (which make up a significant fraction of total P) due to dreissenid grazing than any decrease in dissolved phosphate, for which there are much fewer published measurements than there are for total P. Pothoven and Fahnenstiel (2013) presented data showing that the seston C:P ratio increased following the establishment of dreissenids in Lake Michigan, inferring

increased phosphorus limitation. By comparison, the seston C:P ratios measured in this study are more similar to the pre-dreissenid values reported by Pothoven and Fahnenstiel (2013). This observation, along with that of relatively high P:B ratios reported here, suggests that phosphorus limitation of phytoplankton is not as extreme now as it was shortly following the expansion of quagga mussels in the lake. The reasons for this apparent transition are unclear. Although spring TP and particulate phosphorus have been steadily declining in Lake Michigan for decades, spring total dissolved phosphorus (TDP) concentrations have been relatively stable since 2000 (Barbiero et al., 2018), indicating that the decrease in TP is due mostly to a loss of particulate P. The loss of particulate P over time is likely due to the filtration activities by mussels, but high mussel nutrient excretion rates may be maintaining dissolved nutrients and phytoplankton growth rates. Phytoplankton appear to be growing at the same rate as in the past, or even greater during the spring. But these growth rates are now countered by high loss rates due to dreissenid grazing, resulting in low biomass. While light and temperature appear to play a strong role in driving seasonal patterns of primary production, production is the product of growth rate and biomass. By reducing the biomass, dreissenid grazing has resulted in primary production rates that are likely lower than they would be in the current light / nutrient environment in the absence of dreissenid grazing. The difference in post-dreissenid seston C:P ratios observed in this study and those reported by Pothoven and Fahnenstiel (2013) suggest that the relative influence of dreissenid grazing and nutrient recycling on phytoplankton abundance and nutrient status may have changed over the past decade, and Lake Michigan continues to be an ecosystem in transition.

Conclusions. This study highlights the spatial and seasonal variability of phytoplankton production in Lake Michigan. Productivity and P:B ratios are highly variable from nearshore to

offshore and south to north, suggesting caution when extrapolating measurements from a limited region to the entire lake. Due to the loss of spring and early summer production resulting from mussel grazing during isothermal mixing, production now peaks in August and September, when surface temperatures are warmest. Most production is now concentrated within the epilimnion, and DCL production has decreased. Spring growth rates, as inferred from P:B ratios, appear to have increased following the mussel invasion, perhaps due to increased water clarity and dissolved nutrients excreted by mussels. Summer nutrient limitation, as inferred from seston C:P, and summer growth rates, as inferred from P:B, are similar to what they were before the mussel invasion, suggesting decreased phytoplankton production in Lake Michigan is due mainly to decreases in biomass resulting from dreissenid grazing, rather than increases in nutrient limitation. The decrease in production, along with a shift to increased dominance by picoplankton, likely has implications for energy flow to upper trophic levels.

Acknowledgements

This material is based on work supported by Wisconsin Sea Grant (Grant #R/HCE-28) and the National Science Foundation (Grant #OCE-1658390). We owe thanks the US EPA Great Lakes National Program Office for their partial support through the Great Lakes Restoration Initiative under EPA Contract #EP-W-14-004 and GSA Contract #GS00Q14OADU116, Task Order #47QFLA22F0075, with General Dynamics Information Technology, Inc., directed by Kenneth Klewin and Louis Blume.

We also thank the R/V *Lake Guardian* and R/V *Neeskay* crews for their assistance collecting samples on multiple surveys, and Will Stacy, Jeff Houghton, Pat Anderson, Randy Metzger, and Gerald Becker for help with lab work, fieldwork, and instrumentation. This paper benefited from

the comments of Erica Young, Laodong Guo, Elizabeth Hinchey-Malloy, Annie Scofield, and from the suggestions made by three anonymous reviewers.

References

Babin, M., Morel, A., Gagnon, R., 1994. An incubator designed for extensive and sensitive measurements of phytoplankton photosynthetic parameters. Limnol. Oceanog. 19(3):694-702.

Barbiero, R.P., Lesht, B.M., Warren, G.J., 2012. Convergence of trophic state and the lower food web in Lakes Huron, Michigan and Superior. J. Great Lakes Res. 38, 368–380. https://doi.org/10.1016/j.jglr.2012.03.009

Barbiero, R.P., Lesht, B.M., Warren, G.J., Rudstam, L.G., Watkins, J.M, Reavie, E.D., Kovalenko, K.E., Karatayev, A.Y., 2018. A comparative examination of recent changes in nutrients and lower food web structure in Lake Michigan and Lake Huron. J. Great Lakes Res. 44(4), 573-589, https://doi.org/10.1016/j.jglr.2018.05.012.

Barbiero, R.P., Rudstam, L.G., Watkins, J.M., Lesht, B.M., 2019. A cross-lake comparison of crustacean zooplankton communities in the Laurentian Great Lakes, 1997-2016. J. Great Lakes Res., 45(3), 672-690. https://doi.org/10.1016/j.jglr.2019.03.012.

Bennion, D.H., Warner, D.M,, Esselman, P.C., Hobson, B., Kieft, B., 2019. A comparison of chlorophyll a values obtained from an autonomous underwater vehicle to satellite-based measures for Lake Michigan. J. Great Lakes Res., 45, 726-734. https://doi.org/10.1016/j.jglr.2019.04.003.

Binding, C.E., Greenberg, T.A., Watson, S.B., Rastin, S., Gould, J., 2015. Long term water clarity changes in North America's Great Lakes from multi-sensor satellite observations. Limnol. Oceanogr. 60, 1976-1995. https://doi.org/10.1002/lno.10146

Bootsma, H.A., Liao, Q., 2014. Nutrient cycling by dreissenid mussels: controlling factors and ecosystem response. In, Nalepa, T.F and D.W. Schloesser (eds.) Quagga and Zebra Mussels: Biology, Impacts, and Control (2nd Edition), Taylor and Francis, 555-574.

Bravo H.R., Bootsma, H.A., Khazaei, B, 2019. Fate of phosphorus from a point source in the Lake Michigan nearshore zone. J. Great Lakes Res., 45(6), 1182-1196, https://doi.org/10.1016/j.jglr.2019.09.007.

Bukata, R.P., Jerome, J.H., Bruton, J.E.,1988. Relationships among Secchi disk depth, beam attenuation coefficient, and irradiance attenuation coefficient for Great Lakes waters. J. Great Lakes Res. 14, 347-355.

Bunnell, D.B.,Barbiero, R.P., Ludsin, S.A., Madenjian, C.P., Warren, G.J., Dolan, D.M., Benden, T.O., Briland, R., Gorman, O.T., He, J.X., Johengen, T.H., Lantry, B.F., Lesht, B.M., Nalepa, T.F., Riley, S.C., Riseng, C.M., Treska, T.J., Tsehaye, J., Walsh, M.G., Warner, D.M., Weidel, B.C., 2014. Changing ecosystem dynamics in the Laurentian Great Lakes: bottom-up and top-down regulation. Bioscience, 64(1), 26-39, https://doi.org/10.1093/bioscie/bit001.

Bunnell, D.B., Carrick, H.J., Madenjian, C.P., Rutherford, E.S., Vanderploeg, H.A., Barbiero, R.P., Hinchey-Malloy, E., Pothoven, S.A., Riseng, C.M., Elgin, A.K., Bootsma, H.A., Turschak, B.A., Pangle, K.L., Claramunt, R.M., Czesny, S.J., 2018. Are Changes in Lower Trophic Levels Limiting Prey-Fish Biomass and Production in Lake Michigan? Great Lakes Fishery Commission, Technical Report 2018-1, 42p.

Bunnell, D.B., Ludsin S.A., Knight, R.L., Rudstam, L.G., Williamson, C.E., Hook, T.O.,Collingsworth, P.D., Lesht, B.M., Barbiero, R.P., Scofield, A.E., Rutherfored, E.S., Gaynor, L., Vanderploeg, H.A., Koops, M.A., 2021. Consequences of changing water clarity on the fish ad fisheries of the Laurentian Great Lakes. Can. J. Fish. Aquatic Sci. 78, 1-29, https:dx.doi.org/10.1139/cjfas-2020-0376.

Cai, M., Reavie, E.D., 2018. Pelagic zonation of water quality and phytoplankton in the Great Lakes. Limnology 19, 127–140. https://doi.org/10.1007/s10201-017-0526-y

Carrick H.J., Fahnenstiel G.L., Stoermer E.F., Wetzel R.G. 1991. The importance of zooplankton-protozoan trophic couplings in Lake Michigan. Limnol. Oceanogr. 36,1335-1345. https://doi.org/10.4319/lo.1991.36.7.1335

Carrick, H.J., Butts, E., Daniels, D., Fehringer, M., Frazier, C., Fahnenstiel, G.L., Pothoven, S., Vanderploeg, H.A., 2015. Variation in the abundance of pico, nano, and microplankton in Lake Michigan: Historic and basin-wide comparisons. J. Great Lakes Res. 41, 66–74. https://doi.org/10.1016/j.jglr.2015.09.009.

Chapra, S.C., Dolan, D.M., 2012. Great Lakes total phosphorus revisited: 2. Mass balance modeling. J. Great Lakes Res. 38, 741–754. https://doi.org/10.1016/j.jglr.2012.10.002

Cuhel, R.L., Aguilar, C., 2013. Ecosystem Transformations of the Laurentian Great Lake Michigan by Nonindigenous Biological Invaders. Annu. Rev. Mar. Sci 5, 289–320. https://doi.org/10.1146/annurev-marine-120710-100952

Dove, A., Chapra, S.C., 2015. Long-term trends of nutrients and trophic response variables for the Great Lakes. Limnol. Oceanogr., 60(2), 696-721. https://doi.org/10.1002/lno.10055.

Driscoll, Z.G., Bootsma, H.A., Christiansen, E., 2015. Zooplankton trophic structure in Lake Michigan as revealed by stable carbon and nitrogen isotopes. J. Great Lakes Res., 41 (Sup. 3), 7-15, https://doi.org/10.1016/j.jglr.2015.03.023.

Eadie, B.J., Chambers, R.L., Gardner, W.S., Bell, G.L., 1984. Sediment trap studies in Lake Michigan: resuspension and chemical fluxes in the southern basin. J. Great Lakes Res., 10(3), 307-321.

Eadie, B.J., Schwab, D.J., Johengen, T.H., Lavrentyev, P.J., Miller, G.S., Holland, R.E., Leshkevich, G.A., Lansing, M.B., Morehead, N.R., Robbins, J.A., Hawley, N., Edgington, D.N., Van Hoof, P.L., 2002. Particle transport, nutrient cycling, and algal community structure associated wth a major winter-spring sediment resuspension event in southern Lake Michigan. J. Great. Lakes Res. 28, 324–337.

Edwards, K.F., Thomas, M.K., Klausmeier, C.A., Litchman, E., 2015. Light and growth in marine phytoplankton: Allometric, taxonomic, and environmental variation. Limnol. Oceanogr. 60, 540–552. https://doi.org/10.1002/lno.10033

Engevold, P.M., Young, E.B., Sandgren, C.D., Berges, J.A., 2015. Pressure from top and bottom: lower food web responses to changes in nutrient cycling and invasive species in western Lake Michigan. J. Great Lakes Res., 41(Sup.3), 86-94,

https://doi.org/10.1016/j.jglr.2015.04.015.

Fahnenstiel, G.L., Chandler, J., Carrick, H., Scavia, D., 1989. Photosynthetic characteristics of phytoplankton communities in Lakes Huron and Michigan: PI parameters and end-products. J. Great Lakes Res. 15, 394–407.

Fahnenstiel, G.L., Pothoven, S., Vanderploeg, H., Klarer, D., Nalepa, T., Scavia, D., 2010. Recent changes in primary production and phytoplankton in the offshore region of southeastern Lake Michigan. J. Great Lakes Res. 36, 20–29. https://doi.org/10.1016/j.jglr.2010.03.009

Fahnenstiel, G.L., Scavia, D., 1987a. Dynamics of Lake Michigan Phytoplankton: Primary Production and Growth. Can. J. Fish. Aquat. Sci. 44(3), 499-508. https://doi.org/10.1139/f87-062

Fahnenstiel, G.L., Scavia, D., 1987b. Dynamics of Lake Michigan Phytoplankton: The Deep Chlorophyll Layer. J. Great Lakes Res. 13, 285–295.

Fahnenstiel, G.L., Carrick, H.J., 1988. Primary production in lakes Huron and Michigan: In vitro and in situ comparisons. J. Plankton Res. 10, 1273–1283. https://doi.org/10.1093/plankt/10.6.1273

Fahnenstiel, G.L., Chandler, J.F., Carrick, H.J., Scavia, D., 1989. Photosynthetic characteristics of phytoplankton communities in Lakes Huron and Michigan: P-I parameters and end-products. J. Great Lakes Res. 15, 394–407. https://doi.org/10.1016/S0380-1330(89)71495-7

Fahnenstiel, G.L., Sayers, M.J., Shuchman, R.A., Yousef, F., Pothoven, S.A., 2016. Lake-wide phytoplankton production and abundance in the Upper Great Lakes: 2010-2013. J. Great Lakes Res. 42, 619–629. https://doi.org/10.1016/j.jglr.2016.02.004

Fahnenstiel, G.L., Stone, R. A, McCormick, M.J., Schelske, C.L., Lohrenz, S.E., 2000. Spring isothermal mixing in the Great Lakes: evidence of nutrient limitation and nutrient-light interactions in a suboptimal light environment. Can. J. Fish. Aquat. Sci. 57, 1901–1910. https://doi.org/10.1139/f00-144

Fee, E., 1973a. A numerical model for determining integral primary production and its application to Lake Michigan. J. Fish. Res. Board Canada. 30(10), 1447-1468.

https://doi.org/10.1139/f73-235, https://doi.org/10.1139/f73-236.

Fee, E., 1973b. Modeling primary production in water bodies - numerical approach that allows vertial inhomogeneities. J. Fish. Res. Board Canada. 30(10), 1469-1473.

Fee, E.J., 1990. Computer programs for calculating in situ phytoplankton photosynthesis. Can.Tech.Report Fish.Aquat.Sci. 1740, 1–27.

Gay, D.M., 1990. Usage summary for selected optimization routines. Comput. Sci. Tech. Rep. 153, 1–21.

Geider, R.J., 1987. Light and temperature dependence of the carbon to chlorophyll a ratio in microalgae and cyanobacteria: implications for physiology and growth of phytoplankton. New Phytologist, 106(1), 1-34, https://doi.org/10.1111/J.1469-8137.1987.tb04788.x.

Geider, R.J., Osborne, B.A., 1992. Algal Photosynthesis: the measurement of algal gas exchange. Chapman and Hall, New York.

Grosse, J., van Breugel, P., Boschker, H.T., 2015. Tracing carbon fixation in phytoplankton - compound specific and total ^{13}C incorporation rates. Limno. Oceanogr. Methods, 13(6):288-302.

Haffner, G.D., Griffith, M, Hebert, P.D.N., 1984. Phytoplankton community structure and distribution in the nearshore zone of Lake Ontario. Hydrobiologica, 114(1), 51-66, https://doi.org/10.1007BF00016601.

Hama, T., Miyazaki, T., Ogawa, Y., Iwakuma, T., Takahashi, M., Otsuki, A., Ichimura, S., 1983. Measurement of photosynthetic production of a marine phytolankton population using a stable ^{13}C isotope. Mar. Biol. 73, 31–36.

Harding, L.W., Fisher, T.R., Tyler, M.A., 1987. Adaptive Responses of Photosynthesis in Phytoplankton : Specificity to Time-Scale of Change in Light 4, Biological Oceanography 4(4): 403-438.

Healy, F.P., and Hendzel., L.L., 1980. Physiological indicators of nutrient deficiency in lake phytoplankton. Can. J. Fish. Aquat. Sci. 37, 442-453.

Hecky, R.E., Smith, R.E.H., Barton, D.R., Guildford, S.J., Taylor, W.D., Charlton, M.N.,

Howell, T., 2004. The nearshore phosphorus shunt: a consequence of ecosystem engineering by dreissenids in the Laurentian Great Lakes. Can. J. Fish. Aquat. Sci 61, 1285–1293. https://doi.org/10.1139/F04-065

Hessen, D.O., Andersen, T., Brettum, P., Faafeng, B.A., 2003. Phytoplankton contribution to sestonic mass and elemental ratios in lakes: Implications for zooplankton nutrition. Limnol. Oceanogr. 48, 1289–1296. https://doi.org/10.4319/lo.2003.48.3.1289

Kagami, M. and Urabe, J., 2001. Phytoplankton growth rate as a function of cell size: an experimental test in Lake Biwa. Limnology, 2(2), 111-117.

Klump, J.V., Edgington, D.N., Sager, P.E., Robertson, D.M., 1997. Sedimentary phosphorus cycling and a phosphorus mass balance for the Green Bay (Lake Michigan) ecosystem. Can. J. Fish. Aquat. Sci. 54, 10-26. https://doi.org/10.1139/f96-247

Lampert, W., 1987. Laboratory studies on zooplankton-cyanobacteria interactions Laboratory studies on zooplankton-cyanobacteria interactions. New Zeal. J. Mar. Freshw. Res. 213, 483–490. https://doi.org/10.1080/00288330.1987.9516244

Larsson, U., Nyberg, S. Walve, J., 2021. Phytoplankton primary production: 14C-in situ and 14C-incubator methods compared. ICES J. Mar. Sci. 78(1):3592.3602. https://doi.org/10.10932/icesjms/fsab195.

Lee, S.H., Whitledge, T.E., 2005. Primary and new production in the deep Canada Basin during summer 2002. Polar Biology, 28(3):190-197.

Lee, Z., Marra, J., Perry, M.J., Kahru, M., 2015. Estimating oceanic primary productivity from ocean color remote sensing: A strategic assessment. J. Mar. Syst. 149, 50–59. https://doi.org/10.1016/j.jmarsys.2014.11.015

Lesht, B.M., Barbiero, R.P., Warren, G.J., 2013. A band-ratio algorithm for retrieving open-lake chlorophyll a values from satellite observations of the Great Lakes. J. Great Lakes Res. 39(1):138-152.

Lesht, B.M., Barbiero, R.P., Warren, G.J. 2016. Verification of a simple band-ratio algorithm for retrieving Great Lakes open water surface chlorophyll a concentration from satellite observations. J. Great Lakes Res, 42(2):448-454.

Lohrenz, S.E., Fahnenstiel, G.L, Millie, D.F., Schofield, O.M.E., Johengen, T.H., Bergman, T. Spring phytoplankton photosynthesis, growth, and primary production and relationship to a recurrent coastal sediment plume and river inputs in southeastern Lake Michigan, 2004. J. Geophys. Res., 109(C10S14), 13pp. https://doi.org/10.1029/2004JC00283.

López-Sandoval, D.C., Delgado-Huertas, A., Agusti, S., 2018. J. Plankton Res. 40(5):544-554. https://doi.org/10.1093/plankt/fby031.

Madenjian, C.P., Bunnell, D.B., Warner, D.M., Pothoven, S.A., Fahnenstiel, G.L., Nalepa, T.F., Vanderploeg, H.A., Tsehaye, I., Claramunt, R.M., Clark, R.D., 2015. Changes in the Lake Michigan food web following dreissenid mussel invasions: A synthesis. J. Great Lakes Res. 41, 217–231. https://doi.org/10.1016/j.jglr.2015.08.009

Malkin, S.Y., Guildford, S.J., Hecky, R.E., 2008. Modeling the growth response of *Cladophora* in a Laurentian Great Lake to the exotic invader *Dreissena* and to lake warming. Limnol. Oceanogr. 53, 1111–1124. https://doi.org/10.2307/40058223

Marra, J. 2009. Net and gross productivity: weighing in with ^{14}C. Aquat. Microb. Ecol. 56:123-131.

Mida, J.L, Scavia, D., Fahnenstiel, G.L., Pothoven, S.A., Vanderploeg, H.A., Dolan, D.M., 2010. Long-term and recent changes in southern Lake Michigan water quality with implications for present trophic status. J. Great Lakes Res., 36(Sup. 3), 42-49. https://doi.org/10.1016/j.jglr.2010.03.010.

Millie, D.F., Fahnenstiel, G.L., Lohrenz, S.E., Carrick, H.J., Johengen, T.H., Schofield, O.M.E, 2003. Physical-biological coupling in southern Lake Michigan: influence of episodic sediment resuspension on phytoplankton. Aquatic Ecol., 37(4), 393-408, https://doi.org/10.1012/B:AECO.00000007046.48995.70.

Milligan, A.J., Halsey, K.H., Behrenfeld, M.J., 2015. Advancing interpretations of ^{14}C-uptake measurements in the context of phytoplankton physiology and ecology. J. Plankton Res. 37(4):692-698. https://doi.org/10.1093/plankt/fbv051.

Mosley, C., Bootsma, H., 2015. Phosphorus recycling by profunda quagga mussels (Dreissena

rostriformis bugensis) in Lake Michigan. J. Great Lakes Res. 41, 38–48. https://doi.org/10.1016/j.jglr.2015.07.007

Nalepa, T.F., Fanslow, D.L., Lang, G.A., Mabrey, K., Rowe, M., 2014. Lake-wide benthic surveys in Lake Michigan in 1994-95, 2000, 2005, and 2010: Abundances of the amphipod Diporeia spp. and abundances and biomass of the mussels Dreissena polymorpha and Dreissena rostriformis bugensis, NOAA Technical Memorandum (TM-164) NOAA/GLERL, Ann Arbor, MI.

Nalepa, T.F., Schloesser, D.W. (Eds.), 2013. Quagga and Zebra Mussels: Biology, Impacts, and Control. CRC Press, Boca Raton, FL. ISBN-13: 978-143985436. 815pp.

NASA Goddard Space Flight Center, Ocean Ecology Laboratory, Ocean Biology Processing Group. Moderate-resolution Imaging Spectroradiometer (MODIS) Aqua Ocean Color Data; 2018 Reprocessing. NASA OB.DAAC, Greenbelt, MD, USA. doi: data/10.5067/AQUA/MODIS/L2/OC/2018.

Ozersky, T., Malkin, S.Y., Barton, D.R., Hecky, R.E., 2009. Dreissenid phosphorus excretion can sustain *C. glomerata* growth along a portion of Lake Ontario shoreline. J. Great Lakes Res., 35(3), 321-328, https://doi.org/10.1016/j.jglr.2009.05.001.

Pilcher, D.J., McKinley, G.A., Bootsma, H.A., Bennington, V., 2015. Physical and biogeochemical mechanisms of internal carbon cycling in Lake Michigan. J. Geophys. Res. Oceans, 120(3), 2112-2128, https://doi.org/10.1002/2014JC010594.

Platt, T., Gallegos, C., Harrison, W., 1980. Photoinhibition of photosynthesis in natural assemblages of marine phytoplankton. J. Mar. Res. 38, 687–701.

Platt, T., Jassby, A.D., 1976. The relationship between photosynthesis and light for natural assemblages of coastal marine phytoplankton. J. Phycol. 12, 421–430.

Plattner, S., Mason, D.M., Leshkevich, G.A., Schwab, D.J., Rutherford, E.S., 2006. Classifying and Forecasting Coastal Upwellings in Lake Michigan Using Satellite Derived Temperature Images and Buoy Data. J. Great Lakes Res. 32, 63–76. https://doi.org/10.3394/0380-1330(2006)32[63:CAFCUI]2.0.CO;2

Pothoven, S.A., Fahnenstiel, G.L., 2013. Recent change in summer chlorophyll a dynamics of

southeastern Lake Michigan. J. Great Lakes Res. 39, 287–294. https://doi.org/10.1016/j.jglr.2013.02.005

Rao ,Y.R., Schwab, D.J., 2007. Transport and mixing between the coastal and offshore waters in the Great Lakes: a review. J. Great Lakes Res., 33(1), 202-218.

Reavie, E.D., Barbiero, R.P., Allinger, L.E., Warren, G.J., 2014. Phytoplankton trends in the Great Lakes, 2001-2011. J. Great Lakes Res. 40, 618–639. https://doi.org/10.1016/j.jglr.2014.04.013

Reavie, E.D., Sgro, G.V., Estepp, L.R., Bramburger, A.J., Chraïbi, V.L.S., Pillsbury, R.W., Cai, M., Stow, C.A., Dove, A., 2017. Climate warming and changes in *Cyclotella sensu Iato* in the Laurentian Great Lakes, Limnol. Oceanogr. 62(2), 768-783, https://doi.org/10.1002/lno.10459.

Regaudie-de-Gioux, A., Lasternas, S., Agusti, S., Duarte, C.M., 2014. Comparing marine primary production estimates through different methods and development of conversion equations. Frontiers in Mar. Sci., 1-19: 1-14. https://doi.org/10.3389/fmars.2014.00019.

Rigler, F.H., 1973. A dynamic view of the phosphorus cycle in lakes. In, Griffith, E.J. Beeton, A., Spencer, J.M., Mitchell, D.T. (eds.), An Environmental Phosphorus Handbook, John Wiley and Sones, New York, pp. 539-572.

Rowe, M., Obenour, D., Nalepa, T., Vanderploeg, H.A., Yousef, F., Kerfoot, W., 2015. Mapping the spatial distribution of the biomass and filter-feeding effect of invasive dreissenid mussels on the winter-spring phytoplankton bloom in Lake Michigan. Freshwater. Biol. 60, 2270–2285.

Scavia, D. 1979. Examination of phosphorus cycling and control of phytoplankton dynamics of Lake Ontario with an ecological model. J. Fish. Res. Board Canada, 36(11), 1336-1346.

Scavia, D., Fahnenstiel, G.L., 1987. Dynamics of Lake Michigan phytoplankton: Mechanisms controlling epilimnetic communities. J. Great Lakes Res. 13, 103–120.

Scavia, D., Lang, G., Kitchell, J., 1988. Dynamics of Lake Michigan Plankton: A Model Evaluation fo Nutrient Loading, Competition, and Predation. Can. J. Fish Aquat. Sci. 45, 165–177.

Scofield, A.E., Watkins, J.M., Weidel, B.C., Luckey, F. J., Rudstam, L.G., 2017. The deep chlorophyll layer in Lake Ontario: extent, mechanisms of formation, and abiotic predictors. J. Great Lakes Res., 43(5), 782-794. https://doi.org/10.1016/j.jglr.2017.04.003.

Scofield, A.E., Watkins, J.M., Osantowski, E., Rudstam, L.G., 2020. Deep chlorophyll maxima across a trophic state gradient: a case study in the Laurentian Great Lakes. Limnol. Oceanogr., 65(10), 2460-2484, https://doi.org/10.1002/lno.11464.

Shen, C.Q., Liao, Q., Bootsma, H.A., Troy, C.D., Cannon, D., 2018. Regulation of plankton and nutrient dynamics by profundal quagga mussels in Lake Michigan: a one-dimensional model. Hydrobiologica, 815(1), 47-63. https://doi.org/s10750-018-3647-6.

Shuchman, R.A., Sayer, M., Fahnenstiel, G.A., Leshkevich, G., 2013. A model for determining satellite-derived primary productivity estimates for Lake Michigan. J. Great Lakes. Res., 39(Sup. 1), 46-54. https://doi.org/10.1016/j.jglr.2013.05.001.

Silsbe, G.M., Malkin, S.Y., 2015. Phytotools: Phytoplankton Production Tools. R package version 1.0. https://CRAN.R-project.org/package-phytotools.

Senft, W.H., 1978. Dependence of light-saturated rates of algal photosynthesis on intracellular concentrations of phosphorus. Limnol. Oceanogr. 23, 709–718. https://doi.org/10.4319/lo.1978.23.4.0709.

Slawyk, G., Collins, Y., Auclair, J.C. 1977. The use of ^{13}C and ^{15}N isotopes for the simultaneous measurement of carbon and nitrogen turnover rates in marine phytoplankton 1. Limnol. Oceanog. 22(5):925-932.

Stadig, M.H., Collingsworth, P.D., Lesht, B.M., Höök, T.O., 2020. Spatially heterogeneous trends in nearshore and offshore chlorophyll a concentrations in lake Michigan and Huron (1998-2013). Freshwater Biol., 65, 366-378. http://doi.org/10.1111/fwb.13430.

Stainton, M.P., Capel, M.J., Armstrong, F.A.J., 1977. The chemical analysis of fresh water. Fish. Environ. Canada Misc. Spec. Publ. 25, 166.

Sterner, R.W., 2010. In-situ measured primary production in Lake Superior. J. Great Lakes Res., 36(1), 139-149, https://doi.org/10.1016/j.jglr.2009.12.007.

Sterner, R.W., Elser, J.J., Fee, E.J., Guildford, S.J., Chrzanowski, T.H., 1997. The Light: Nutrient Ratio in Lakes: The Balance of Energy and Materials Affects Ecosystem Structure and Process. Am. Nat. 150, 663–684. https://doi.org/10.1086/286088

Sterner, R.W., Hessen, D.O., 1994. Algal nutrient limitation and the nutrition of aquatic herbivores. Annu. Rev. Ecol. Syst 25, 1–29.

Talling, J.F., 1957. Photosynthetic Characteristics of Some Freshwater Plankton Diatoms in Relation To Underwater Radiation. New Phytol. 56, 29–50. https://doi.org/10.1111/j.1469-8137.1957.tb07447.x

Turschak BA, Bunnell D, Czesny S, Höök TO, Janssen J, Warner D, Bootsma HA. 2014. Nearshore energy subsidies support Lake Michigan fishes and invertebrates following major changes in food web structure. Ecology 95(5), 1243-52.

Turschak BA, Bootsma HA. Lake Michigan trophic structure as revealed by stable C and N isotopes. J. Great Lakes Res. 41, 185-96.

Vanderploeg, H.A., Liebig, J.R., Carmichael, W.W., Agy, M.A., Johengen, T.H., Fahnenstiel, G.L., Nalepa, T.F., 2001. Zebra mussel (Dreissena polymorpha) selective filtration promoted toxic Microcystis blooms in Saginaw Bay (Lake Huron) and Lake Erie. Can. J. Fish. Aquat. Sci. 58, 1208–1221. https://doi.org/10.1139/cjfas-58-6-1208

Vanderploeg, H.A., Liebig, J.R., Nalepa, T.F., Fahnenstiel, G.A., Pothoven, S.A., 2010. Dreissena and the disappearance of the spring phytoplankton bloom in Lake Michigan. J. Great Lakes Res., 38(Sup. 3), 50-59. https://doi.org/10.1016/j.jglr.2010.04.005.

Vanderploeg, H.A., Pothoven, S.A., Fahnenstiel, G.L., Cavaletto, J.F, Liebig, J.R., Stow, C.A., Nalepa, T.F., Madenjian, C.P., Bunnell, D.B., 2012. Seasonal zooplankton dynamics in Lake Michigan: disentangling impacts of resource limitation, ecosystem engineering, and predation during a critical ecosystem transition. J. Great Lakes Res., 30(2), 336-352, https://doi.org/10.1016/j.jglr.2012.02.005.

U.S. EPA, 2013. Standard Operating Procedure for Chlorophyll a Sampling (LG404) Version 7. Great Lakes National Program Office, March 7, 2013.

U.S. EPA, 2017. Standard Operating Procedure for Field Sampling Using the Rosette Sampler

(LG200) Version 8. Great Lakes National Program Office, July 8, 2017.

U.S. EPA, 2019. Standard Operating Procedure for GLNPO Board Analysis (LG500) Version 09.01. Great Lakes National Program Office, March, 2019.

U.S. EPA, 2021. Great Lakes Biology Monitoring Program Technical Report: Status and Trends through 2018 for Chlorophyll, Phytoplankton, Zooplankton, *Mysis*, and Benthos. (EPA 950-R-20-008).

Waples, J.T., H.A. Bootsma, and J.V. Klump. 2016. How are coastal benthos fed? Limnol. Oceanogr. Letters 2(1):18-28. doi: 10.1002/lol2.10033.

Ware, D., Thomson, R., 2005. Bottom-up ecosystem trophic dynamics determine fish production in the Northeast Pacific. Science, 308, 1280-1284, https://doi.org/10.1126/SCIENCE.11

Warner, D.M., Lesht, B.M., 2015. Relative importance of phosphorus, invasive mussels and climate for patterns in chlorophyll a and primary production in Lakes Michigan and Huron. Freshw. Biol. 60, 1029–1043. https://doi.org/10.1111/fwb.12569

Warren, G.J., Lesht, B.M., Barbiero, R.P., 2017. Estimation of the width of the nearshore zone in Lake Michigan using eleven years of MODIS satellite imagery. J. Great Lakes Res. https://doi.org/10.1016/j.jglr.2017.11.011

Webb, W.L., Newton, M., Starr, D., 1974. Carbon Dioxide Exchange of Alnus rubra. A Mathematical Model. Oecologia 17, 281–291.

Welschmeyer, N.A., Lorenzen, C.J., 1981. Chlorophyll-specific photosynthesis and quantum efficient at subsaturating light intensities. J. Phycology, 17(4), 283-293.

Wetzel, R., 2001. Limnology: Lake and river ecosystems, Third. ed. Academic Press, San Diego.

Williams, P.J.L.B., Lefèvre, D., 2008. An assessment of the measurement of phytoplankton respiration rates from dark ^{14}C incubations. Limnol. Oceanogr. Methods 6, 1–11.

Yousef, F., Kerfoot, W.C., Shuchman, R., Fahnenstiel, G., 2014. Bio-optical properties and primary production of Lake Michigan: Insights from 13-years of SeaWiFS imagery. J. Great Lakes Res. 40, 317–324. https://doi.org/10.1016/j.jglr.2014.02.018

Yousef, F., Shuchman, R., Sayers, M., Fahnenstiel, G., Henareh, A., 2017. Water clarity of the

Upper Great Lakes: Tracking changes between 1998–2012. J. Great Lakes Res. 43, 239–247. https://doi.org/10.1016/j.jglr.2016.12.002

Yurista, P.M., Kelly, J.R., Cotter, A.M., Miller, S.E., Van Alstine, J.D., 2015. Lake Michigan: Nearshore variability and a nearshore-offshore distinction in water quality. J. Great Lakes Res. 41, 111–122. https://doi.org/10.1016/j.jglr.2014.12.010

Zhang, H., Culver, D.A., Boegman, L., 2011. Dreissenids in Lake Erie: An algal filter or a fertilizer? Aquat. Invasions 6, 175–194. https://doi.org/10.3391/ai.2011.6.2.07

Tables

Table 1. Summary of stations and sampling. Sample depth abbreviations indicate the deep chlorophyll layer (DCL) identified as the depth of chlorophyll fluorescence maximum, mid-depth (MID), base of epilimnion (LEP), and depth of maximum dissolved oxygen concentration (DO). Samples is the number of incubation experiments done at each station.

Station	Latitude	Longitude	Station Depth (m)	Survey/Dates	Depths Sampled	Samples
AW15	43.0958	-87.8611	15	Transect 2017, see Table 5 for dates	5 or 6 m (October)	3
AW45	43.0980	-87.7840	45	Transect 2017, see Table 5 for dates	5 m, DCL, see Table 5 for depths	6
AW75	43.0979	-87.7187	75	Transect and Time Series 2017, see Tables 4 and 5 for dates	5 m, 35 m (unstratified); 5m, DCL, LEP, or DO (stratified), see Tables 4 and 5 for depths	26
DC75	44.8941	-87.0515	75	Summer 2017, 8/6/2017	8 m, DCL (19 m)	2
GB1	45.3999	-86.7115	40	Summer 2017, 8/7/2017	5 m	1
MI11	42.3833	-87.0000	128	Summer 2017, 8/2/2017	5 m, DCL (37 m)	2
MI17	42.7333	-87.4167	100	Spring 2016, 3/27/2016	2 m, MID (50 m)	2
MI23	43.1333	-87.0000	88	Spring 2016, 3/27/2016, Summer 2017, 8/3/2017	2 m, MID (51 m, spring); 5 m, DCL (39 m, summer)	2 2
MI34	44.0900	-86.7667	160	Spring 2016, 3/26/2016, Summer 2017, 8/5/2017	2 m, MID (78 m, spring); 5 m, DCL (46 m, summer)	2 2
MI41	44.7367	-86.7217	250	Summer 2017, 8/6/2017	5 m, DCL (34 m)	2
MI47	45.1783	-86.3750	186	Spring 2016, 3/28/2016	2 m, MID (35 m)	2
MI52	45.8083	-86.0456	54	Summer 2017, 8/7/2017	5 m, DCL (15 m)	2
MI-N	45.8723	-85.6970	38	Spring 2016, 3/28/2016	2 m, MID (19 m)	2

Table 2. Spring 2016 R/V Lake Guardian survey photosynthetic parameters (± SE), water temperature (°C), chlorophyll a concentration (mg m^{-3}), and integrated production (mg C m^{-2} day^{-1}) calculated using simulated PAR (27.5% cloud cover) for each site and date. Although listed with the shallow samples, the integrated production calculation was based on the P-I parameters determined at both sample depths. Italics indicate manual parameter calculation because model fitting error was significant. Units of P_M^B and P_S^B are mg C mg chl^{-1} hr^{-1}, α^B and β^B are mg C mg chl^{-1} mol photons $^{-1}$ m^2, and I_k and I_b are mol photons m^{-2} hr^{-1}. Values are grouped by sample depth.

Site	Depth	P_M^B	P_S^B	α^B	β^B	I_k	I_b	r^2	Temp	Chl	Prod
MI17	2	*0.88*	-	*3.07*	-	*0.28*	-	0.769	3.25	0.52	201.1
MI23	2	0.96	-	11.8 ± 0.84	-	0.08 ± 0.01	-	0.920	3.42	0.79	337.5
MI34	2	1.05	-	8.03 ± 1.89	-	0.13 ± 0.03	-	0.824	3.50	0.62	253.7
MI47	2	1.24	-	9.84 ± 0.97	-	0.13 ± 0.01	-	0.979	3.47	0.59	243.7
MI-N	2	1.41	-	8.90 ± 1.11	-	0.16 ± 0.02	-	0.862	2.19	0.44	243.3
MI17	50	0.93	1.00 ± 0.04	6.23 ± 0.77	0.08 ± 0.02	0.15	12.4	0.909	3.21	0.48	
MI23	51	1.39	1.54 ± 0.05	14.6 ± 1.85	0.29 ± 0.04	0.10	4.88	0.987	3.42	0.57	
MI34	78	1.51	-	9.84 ± 0.79	-	0.15 ± 0.01	-	0.972	3.49	0.56	
MI47	35	1.49	-	5.36 ± 2.45	-	0.28 ± 0.14	-	0.630	3.42	0.55	
MI-N	19	2.06	-	12.1 ± 0.92	-	0.17 ± 0.01	-	0.973	2.21	0.40	

Table 3. As Table 2 for Summer 2017 R/V Lake Guardian survey. Bold type indicates statistically insignificant β parameter.

Site	Depth	P_M^B	P_S^B	α^B	β^B	I_k	I_b	r^2	Temp	Chl	Prod
MI11	5	0.99	**1.46 ± 0.39**	2.38 ± 0.35	**0.29 ± 0.20**	0.42	**3.37**	0.963	23.4	1.10	316.9
MI23	5	1.89	-	3.09 ± 0.37	-	0.61 ± 0.10	-	0.978	21.9	1.05	447.1
MI34	5	1.07	1.25 ± 0.09	3.09 ± 0.30	0.11 ± 0.05	0.35	9.51	0.989	19.2	1.37	386.5
MI41	5	1.06	1.27 ± 0.15	3.32 ± 0.35	0.15 ± 0.08	0.32	7.23	0.979	19.0	1.94	500.1
DC75	8	1.46	1.79 ± 0.12	4.33 ± 0.31	0.22 ± 0.06	0.34	6.74	0.993	18.8	1.67	545.8
GB1	5	1.07	1.34 ± 0.10	3.81 ± 0.41	0.22 ± 0.06	0.28	4.78	0.986	19.1	2.17	502.2
MI52	5	1.26	1.44 ± 0.10	3.70 ± 0.40	0.11 ± 0.05	0.34	11.6	0.991	18.8	2.06	549.0
MI11	15	1.37	1.52 ± 0.07	4.10 ± 0.20	0.09 ± 0.03	0.33	15.5	0.997	18.8	2.01	
MI23	37	0.53	0.63 ± 0.03	6.25 ± 0.42	0.28 ± 0.03	0.08	1.89	0.991	5.36	1.53	
MI34	39	0.73	0.98 ± 0.15	5.35 ± 0.73	0.45 ± 0.15	0.14	1.60	0.954	5.01	1.40	
MI41	46	0.53	0.63 ± 0.06	7.64 ± 1.04	0.31 ± 0.07	0.07	1.74	0.968	4.76	2.28	
DC75	34	0.50	**0.58 ± 0.10**	6.97 ± 2.00	**0.22 ± 0.10**	0.07	**2.32**	0.862	5.36	3.66	
GB1	19	0.94	1.13 ± 0.18	6.50 ± 1.13	0.30 ± 0.13	0.14	3.15	0.937	10.6	1.58	

Table 4. As Table 2 for 2017 AW75 seasonal survey. Bold type indicates insignificant β parameter, but significant visible photoinhibition. Asterisks indicate a size-fractionated sample for which the parameter values are based on biomass weighted averages of the parameters determined for the three size fractions (see Table 6).

Date	Depth	P_M^B	P_S^B	α^B	β^B	I_k	I_b	r^2	Temp	Chl	Prod
11 May	5	0.45	-	1.89 ± 0.57	-	0.24	-	0.871	4.71	0.77	267.5
	35	0.87	-	5.29 ± 1.24	-	0.16	-	0.960	4.11	0.77	
26 May	5	0.85	-	5.64 ± 0.63	-	0.15 ± 0.02	-	0.951	6.43	0.82	352.1
	35	0.88	0.90 ± 0.02	5.69 ± 0.16	0.02 ± 0.01	0.16	50.2	0.998	6.22	0.84	
08 June	5	1.25	-	5.86 ± 0.59	-	0.21± 0.02	-	0.965	9.79	0.72	380.1
	26	0.66	0.72 ± 0.05	7.73 ± 1.54	0.15 ± 0.04	0.09	4.36	0.884	6.70	1.83	
23 June	5	1.96	-	6.74 ± 0.80	-	0.29 ± 0.04	-	0.972	16.0	1.05	498.0
	27*	0.33	0.41	3.93	0.23	0.08	1.40		6.03	2.74	
11 July	5	1.19	-	5.35 ± 0.76	-	0.22 ± 0.03	-	0.944	18.4	0.91	333.5
	30	0.40	0.44 ± 0.02	6.70 ± 1.05	0.12 ± 0.02	0.06	3.32	0.958	5.60	2.74	
25 July	5	1.57	-	4.45 ± 0.32	-	0.35 ± 0.03	-	0.995	19.9	1.15	407.3
	40*	0.67	0.85	10.2	0.64	0.05	0.75		5.47	3.20	
16 Aug	5	1.47	-	3.23 ± 0.32	-	0.46 ± 0.05	-	0.989	21.3	2.06	568.4
	25	0.88	1.07 ± 0.10	5.25 ± 0.61	0.24 ± 0.07	0.17	3.66	0.950	7.70	1.83	
29 Aug	5	3.13	-	8.85 ± 0.50	-	0.35 ± 0.02	-	0.996	20.1	1.07	685.5
	22	1.91	2.55 ± 0.21	12.3 ± 1.57	1.00 ± 0.21	0.16	1.92	0.978	8.62	1.17	
12 Sep	5	1.75	-	*10.7*	-	*0.16*	-	0.004	18.9	1.60	637.3
	38	1.39	1.63 ± 0.16	16.1 ± 3.28	0.62 ± 0.18	0.09	2.23	0.924	5.91	0.94	
25 Sep	5	2.63	-	7.14 ± 0.90	-	0.37 ± 0.05	-	0.976	21.6	1.14	390.1
	28*	0.74	0.95	7.84	0.53	0.09	1.37		5.82	0.77	
09 Oct	5	3.84	-	14.6 ± 3.38	-	0.26 ± 0.07	-	0.822	14.8	0.89	405.9
	10	2.82	-	13.1 ± 1.79	-	0.22 ± 0.03	-	0.946	14.3	1.00	
23 Oct	5	1.62	**1.99 ± 0.27**	7.21 ± 1.44	**0.36 ± 0.19**	0.23	**4.49**	0.934	12.0	1.48	510.4
	16	2.70	3.27 ± 0.24	22.5 ± 3.03	1.08 ± 0.24	0.12	2.50	0.968	10.6	0.87	
13 Nov	5	0.75	0.81 ± 0.06	6.11 ± 1.47	0.09 ± 0.04	0.12	8.19	0.962	6.09	1.94	323.8
	25	0.95	1.03 ± 0.04	8.93 ± 0.98	0.16 ± 0.03	0.11	6.06	0.987	5.33	0.55	

Table 5. As Table 2 for 2017 transect surveys. Bold type indicates insignificant β parameter, but significant visible photoinhibition. Italics indicate manual parameter calculation because model fitting error was significant.

Site	Depth	P_M^B	P_S^B	α^B	β^B	I_k	I_b	r^2	Temp	Chl	Prod
11 Jul											
AW15	5	2.73	-	8.79 ± 0.51	-	0.31± 0.02	-	0.982	10.5	4.01	1190.2
AW45	5	1.47	-	4.41 ± 0.65	-	0.33 ± 0.06	-	0.875	15.7	1.37	407.1
	22	0.43	**0.48 ± 0.08**	4.12 ± 1.75	**0.09 ± 0.06**	0.11	**4.62**	0.574	6.19	2.86	
AW75	5	1.19	-	5.35 ± 0.76	-	0.22 ± 0.03	-	0.944	18.4	0.91	333.5
	30	0.40	0.44 ± 0.02	6.70 ± 1.05	0.12 ± 0.02	0.06	3.32	0.958	5.60	2.74	
12 Sep											
AW15	5	6.57	-	12.1 ± 0.63	-	0.55 ± 0.04	-	0.998	18.3	2.28	1151.4
AW45	5	2.11	2.50 ± 0.20	4.67 ± 0.34	0.18 ± 0.08	0.45	11.5	0.995	18.6	2.28	876.6
	36	1.84	2.16 ± 0.33	19.1 ± 6.28	0.71 ± 0.34	0.10	6.28	0.804	6.47	0.62	
AW75	5	*1.75*	-	*10.7*	-	*0.16*	-	0.004	18.9	1.60	637.3
	38	1.39	1.63 ± 0.16	16.1 ± 3.28	0.62 ± 0.18	0.09	2.23	0.924	5.91	0.94	
09 Oct											
AW15	6	2.96	-	19.04 ± 4.76	-	0.16 ± 0.04	-	0.575	7.08	0.38	172.7
AW45	5	2.12	-	5.13 ± 1.23	-	0.41 ± 0.11	-	0.847	9.93	0.92	277.3
	17	1.95	2.10 ± 0.11	13.0 ± 1.83	0.18 ± 0.07	0.15	10.7	0.971	7.01	0.68	
AW75	5	3.84	-	14.6 ± 3.38	-	0.26 ± 0.07	-	0.822	14.8	0.89	405.9
	10	2.82	-	13.1 ± 1.79	-	0.22 ± 0.03	-	0.946	14.3	1.00	

Table 6. Size-fractionated photosynthetic parameters (± SE) and chlorophyll concentrations from the depth of maximum fluorescence at Station AW75. Units for variables as in Tables 2-5. Bold type indicates insignificant β parameter, but visible photoinhibition in the P-I curve. Underlined dates indicate a DCL sample.

Date	Size Class	P_M^B	α^B	β^B	I_k	r^2	Chl (%)
23 Jun	< 2 µm	0.36	5.75 ± 1.88	0.14 ± 0.05	0.06	0.890	1.47 (53.8)
(27 m)	2-20 µm	0.29	2.00 ± 0.34	0.21 ± 0.08	0.15	0.954	0.79 (28.8)
	20-200 µm	0.22	1.52 ± 0.13	0.51 ± 0.15	0.14	0.994	0.48 (17.5)
25 Jul	< 2 µm	0.57	15.7 ± 2.57	0.35 ± 0.05	0.04	0.983	1.71 (53.5)
(40 m)	2-20 µm	0.40	1.48 ± 0.23	**1.60 ± 4.16**	0.27	0.965	0.83 (25.9)
	20-200 µm	0.33	7.06 ± 3.88	**0.17 ± 0.09**	0.05	0.770	0.66 (20.6)
25 Sep	< 2 µm	0.67	7.21 ± 0.92	0.56 ± 0.15	0.09	0.979	0.35 (46.2)
(28 m)	2-20 µm	0.86	6.55 ± 0.41	1.12 ± 0.20	0.13	0.994	0.14 (18.0)
	20-200 µm	0.72	9.27 ± 3.24	**0.19 ± 0.11**	0.08	0.761	0.28 (35.8)

Figure Captions:

Figure 1. Locations of Lake Michigan sampling sites. Contour lines are 50 m intervals. Dashed line indicates the boundary between the northern and southern basins.

Figure 2. Measurements made during the whole lake surveys versus the latitude of the sampling stations. The spring survey data are indicated by circles connected by a solid line and the summer survey data are shown as diamonds connected by a dashed line. The panels are (a) surface temperature; (b) chlorophyll a; (c) mean percent surface irradiance (I_0) in the mixed layer; (d) areal production; (e) P:B ratio; and (f) seston C:P ratio. Dotted lines in panel (f) indicate moderate (>129) and severe (> 258) phosphorus deficiency based on the criteria from Healy and Hendzel (1980). Seston carbon was not measured at station MI47 during the spring survey.

Figure 3. Sampled values of chlorophyll *a* at survey stations (diamonds) and from fluorometer (lines) during the spring (panel a) and summer (panel b) on satellite-retrieved estimates of surface chlorophyll *a* concentration. Satellite estimates are based on temporal composites of imagery collected ± 7 days of the sampling dates.

Figure 4. Photosynthesis parameters P_M^B (mg C mg Chl^{-1} hr^{-1}) and α^B (mg C mg Chl^{-1} mol photons^{-1} m^2) in spring (left column) and summer (right column).

Figure 5. Seasonal variation in (a) daily areal production calculated using measured surface PAR from May to November (LOESS smoothing line ± 95% CI represented by shaded area), (b) monthly mean daily areal production (± 1 SD), and variation in daily areal production estimates due to variation in (c) chlorophyll (Chl) and epilimnetic P-I parameters (PI), (d) surface irradiance (I_o) and water clarity (k).

Figure 6. Seasonal variation in epilimnetic and mid-depth chlorophyll, P:B, seston C:P, phytoplankton C:Chl, P_M^B (mg C mg Chl^{-1} hr^{-1}), and α^B (mg C mg Chl^{-1} mol photons $^{-1}$ m^2). Large

gray diamond points indicate mid-depth samples collected in the DCL. Horizontal dotted lines mark nutrient deficiency criteria as defined by Healy and Hendzel (1980).

Figure 7. Seasonal vertical structure of temperature, chlorophyll (as inferred from fluorescence), and phytoplankton production. Vertical lines indicate sampling dates. Linear interpolation was used between sampling dates for temperature and chlorophyll. Production was calculated for each day using P-I parameters, k_{PAR}, and biomass linearly interpolated between dates and simulated PAR (reflectance and constant 26.5% cloud cover).

Figure 8. Proportion of the total water column production at station AW75 found within the epilimnion, below the epilimnion, and within the deep chlorophyll layer (DCL, that section of the water column in which chlorophyll > 2 mg m^{-3}) during the stratified period.

Figure 9. Vertical structure of temperature, corrected CTD chlorophyll, and phytoplankton production calculated using simulated PAR (reflectance and constant 26.5% cloud cover) on July 11, 2017, at Stations AW15 (0.25 km offshore), AW45 (6.5 km offshore), and AW75 (11.5 km offshore). White points represent discrete sampling points for photosynthesis measurements.

Figure 10. As Figure 9 on Sep 12, 2017.

Figure 11. As Figure 9 on Oct 9, 2017.

Figure 12. Optimum PAR level (I_{opt}, PAR value at which photoinhibition begins) versus the light saturation parameter (I_k) for whole-lake and seasonal experiments with observed photoinhibition. Survey is indicated by the symbol shape and sample depth by the size of the symbols.

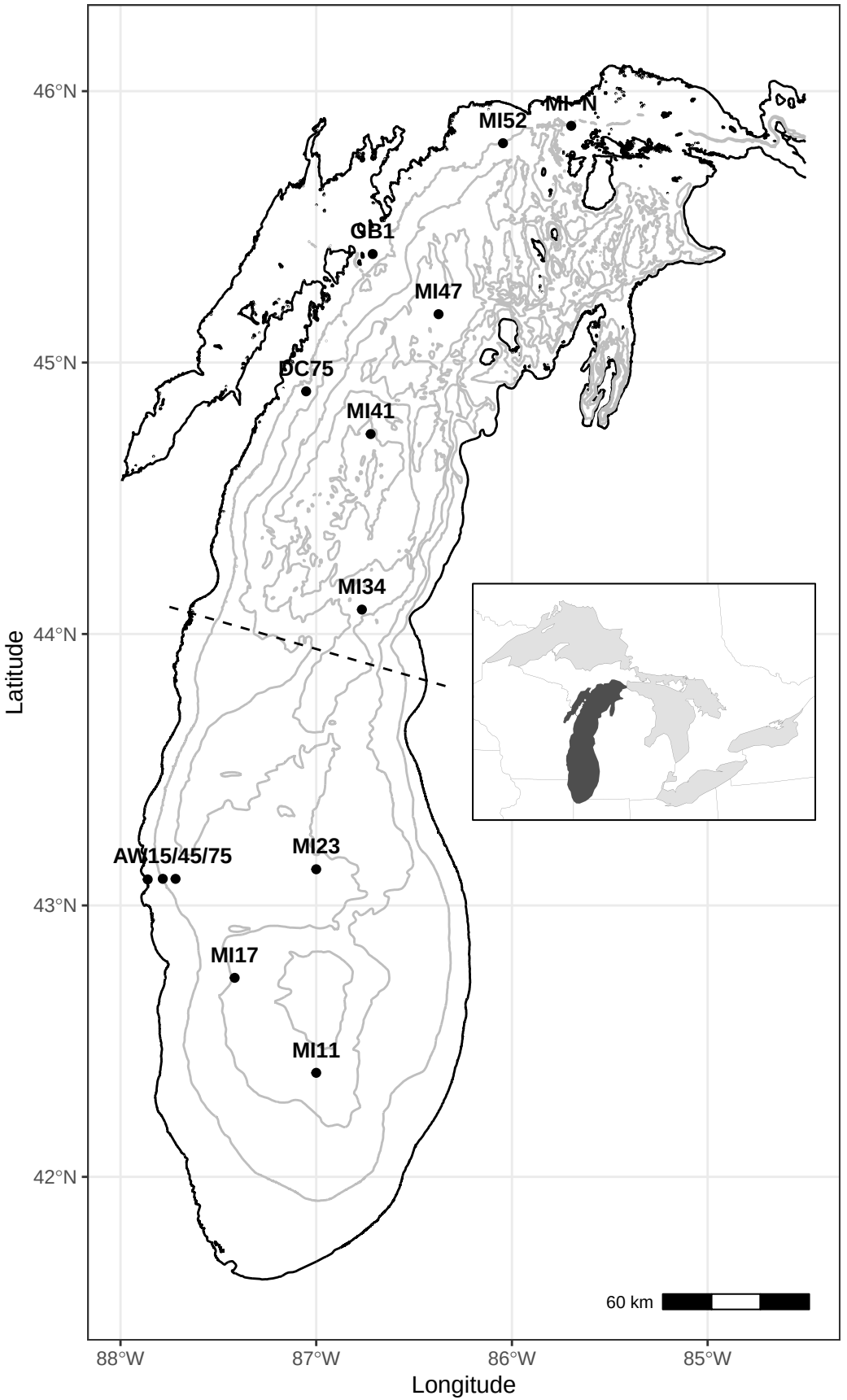
MI52
MI47
MI41
MI34
MI23
MI17
MI11
60 km
46°N
45°N
44°N
43°N
42°N
88°W
87°W
86°W
85°W
Latitude
Longitude

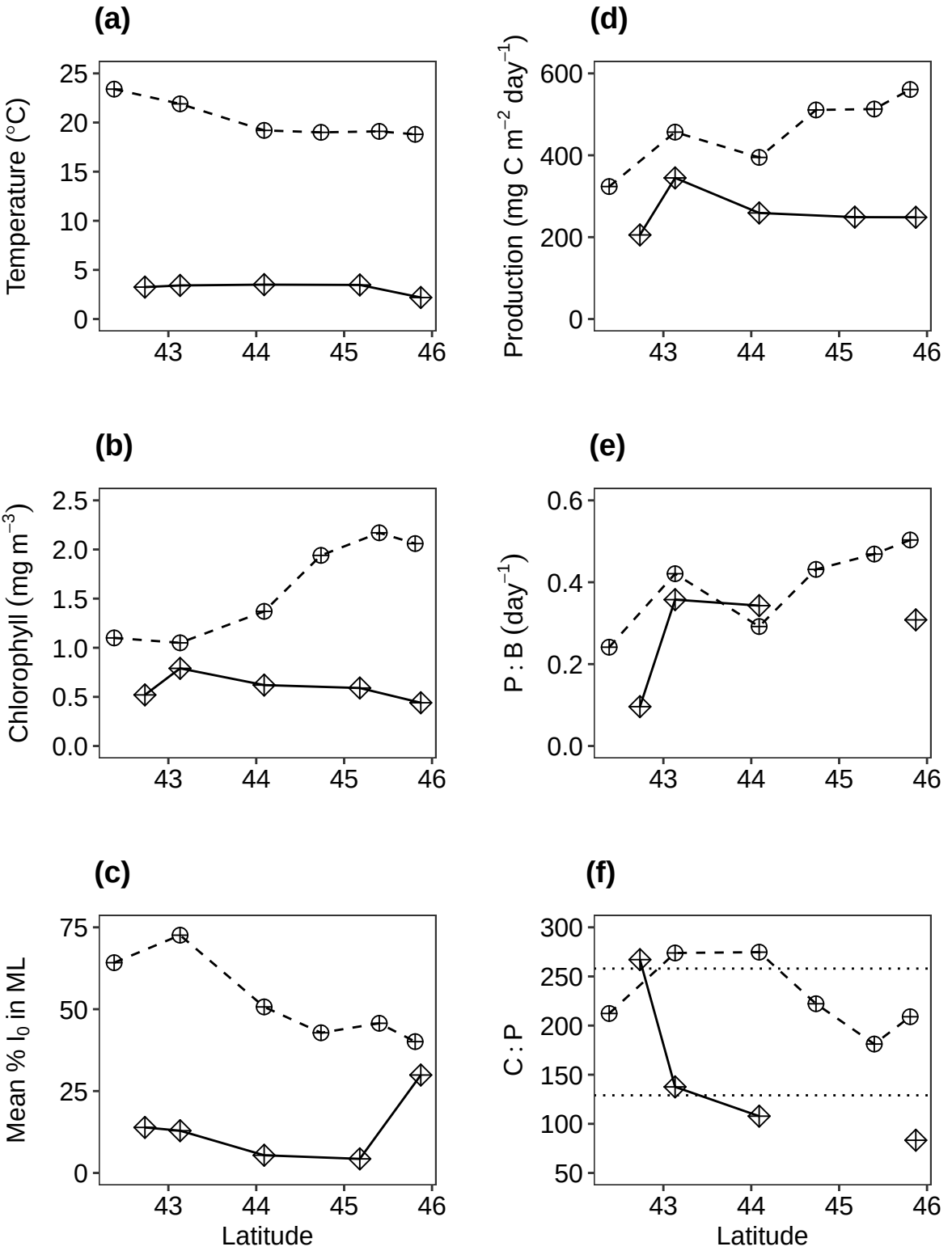
(a)
Temperature (°C)
25
20
15
10
5
0
43
44
45
46
(d)
Production (mg C m^{-2} day^{-1})
600
400
200
0
(b)
Chlorophyll (mg m^{-3})
2.5
2.0
1.5
1.0
0.5
0.0
(e)
P : B (day^{-1})
0.6
0.4
0.2
0.0
(c)
Mean % I_0 in ML
75
50
25
0
Latitude
(f)
C : P
300
250
200
150
100
50
Latitude

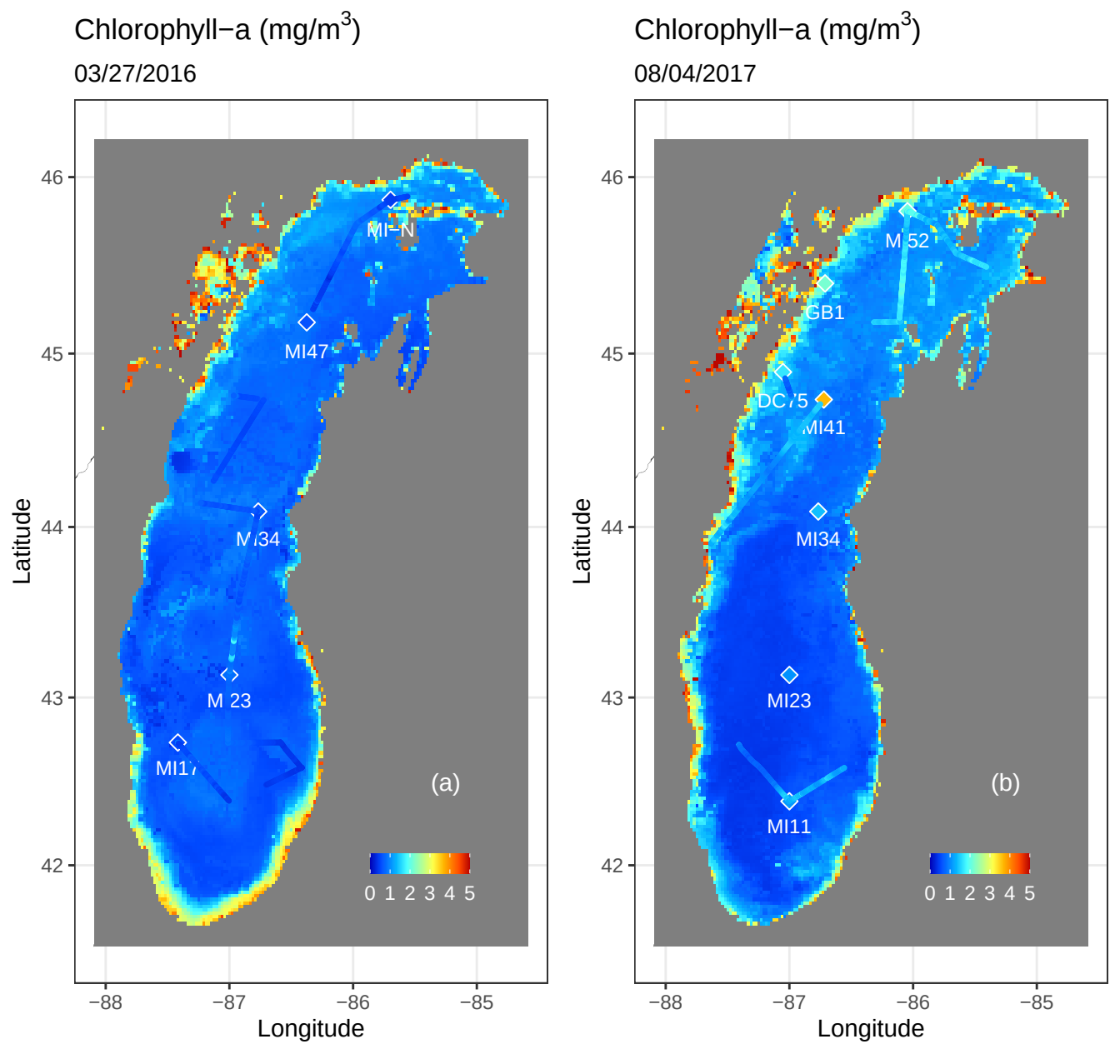
Chlorophyll−a (mg/m3)
03/27/2016
MI−N
MI47
MI34
M 23
MI1
(a)
0 1 2 3 4 5
Latitude
Longitude
46
45
44
43
42
−88
−87
−86
−85
Chlorophyll−a (mg/m3)
08/04/2017
M 52
GB1
DC 5
MI41
MI34
MI23
MI11
(b)
0 1 2 3 4 5
Latitude
Longitude

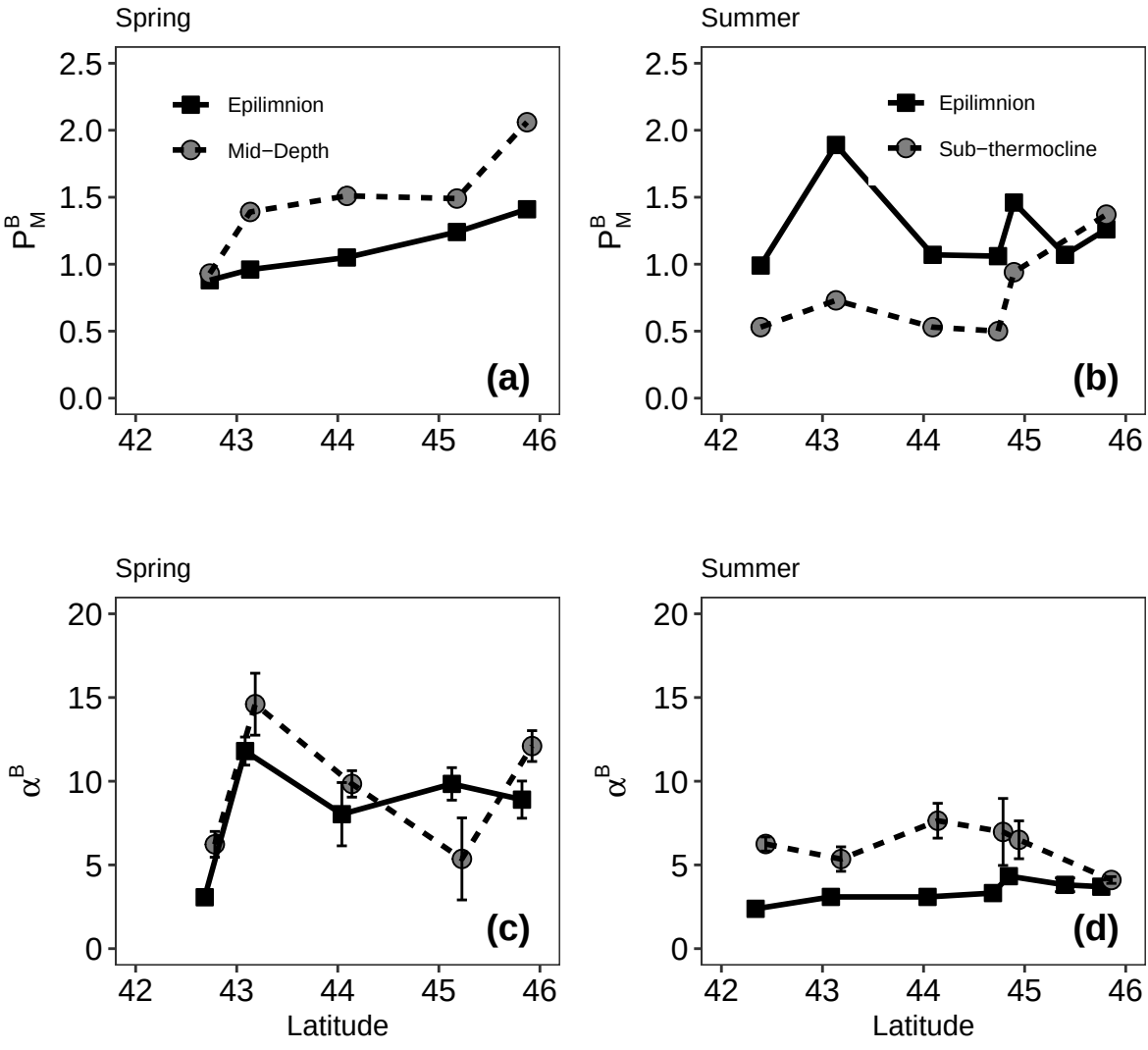
Spring
Summer
Epilimnion
Mid−Depth
Sub−thermocline
P_M^B
α^B
(a)
(b)
(c)
(d)
Latitude
0.0
0.5
1.0
1.5
2.0
2.5
0
5
10
15
20
42
43
44
45
46

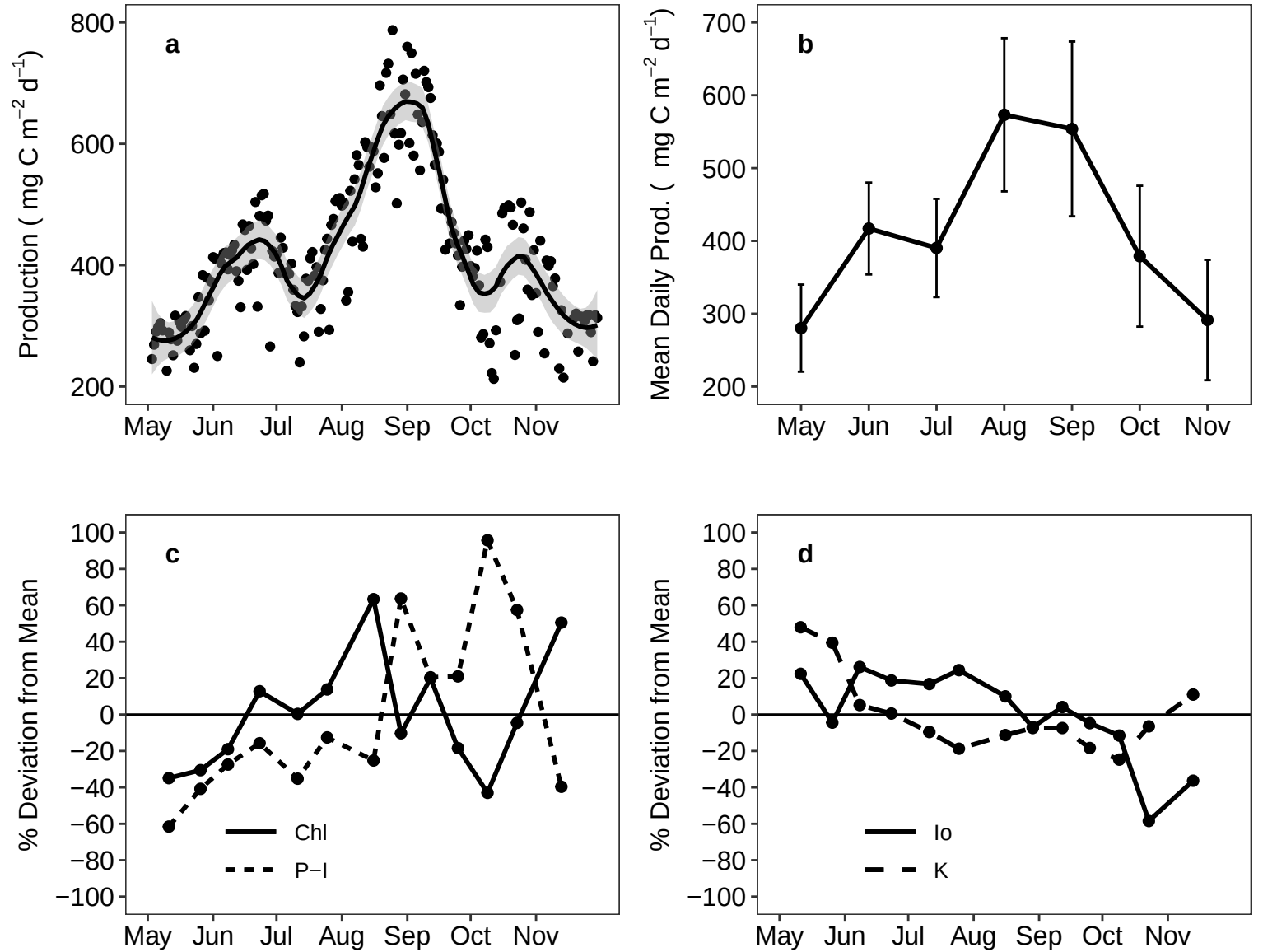
a
b
c
d
Production (mg C m^{-2} d^{-1})
Mean Daily Prod. (mg C m^{-2} d^{-1})
% Deviation from Mean
% Deviation from Mean
800
600
400
200
700
600
500
400
300
200
100
80
60
40
20
0
−20
−40
−60
−80
−100
May
Jun
Jul
Aug
Sep
Oct
Nov
Chl
P−I
Io
K

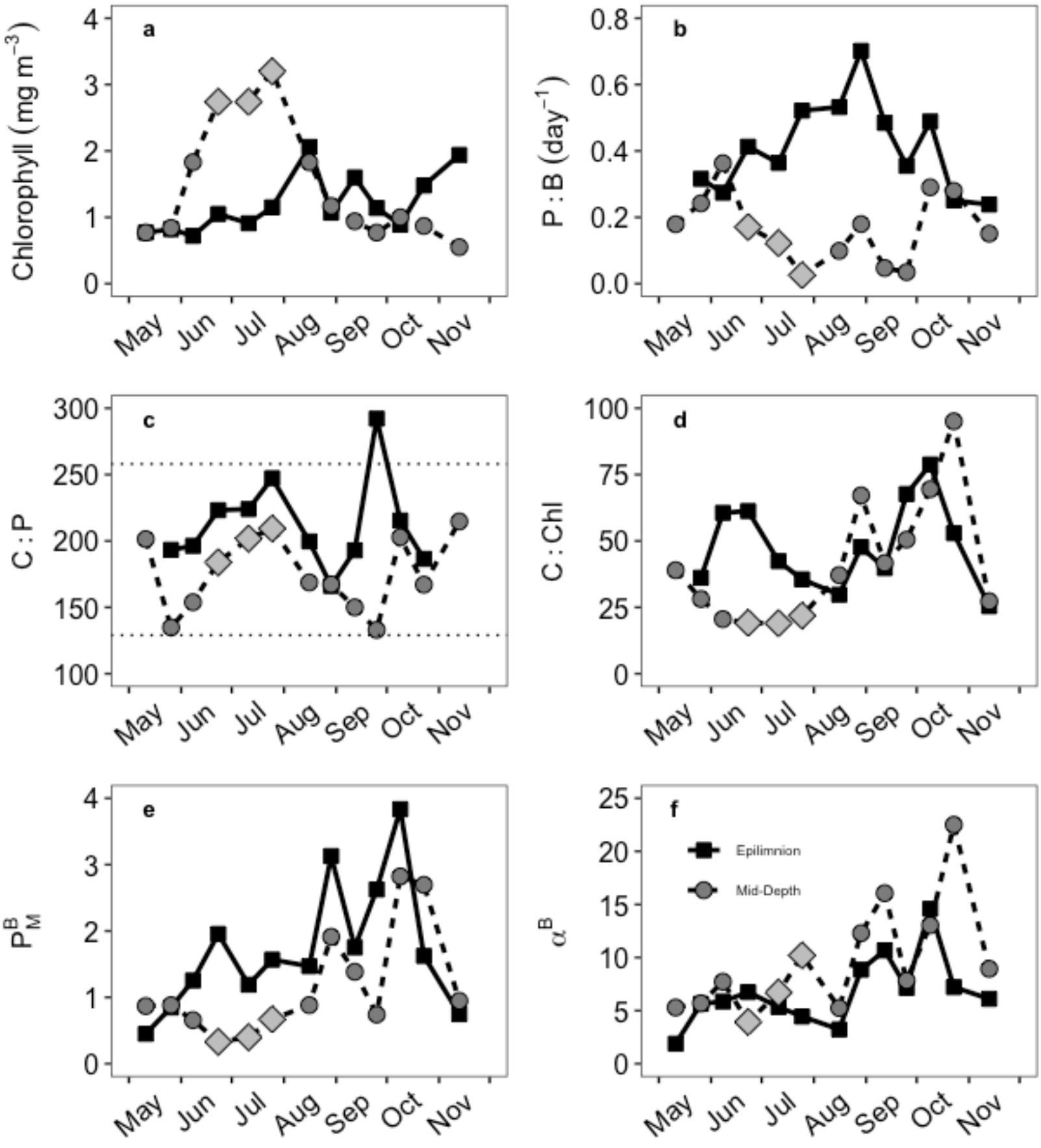
a
b
c
d
e
f
Chlorophyll (mg m^{-3})
P : B (day^{-1})
C : P
C : Chl
P_M^B
α^B
Epilimnion
Mid-Depth
May
Jun
Jul
Aug
Sep
Oct
Nov

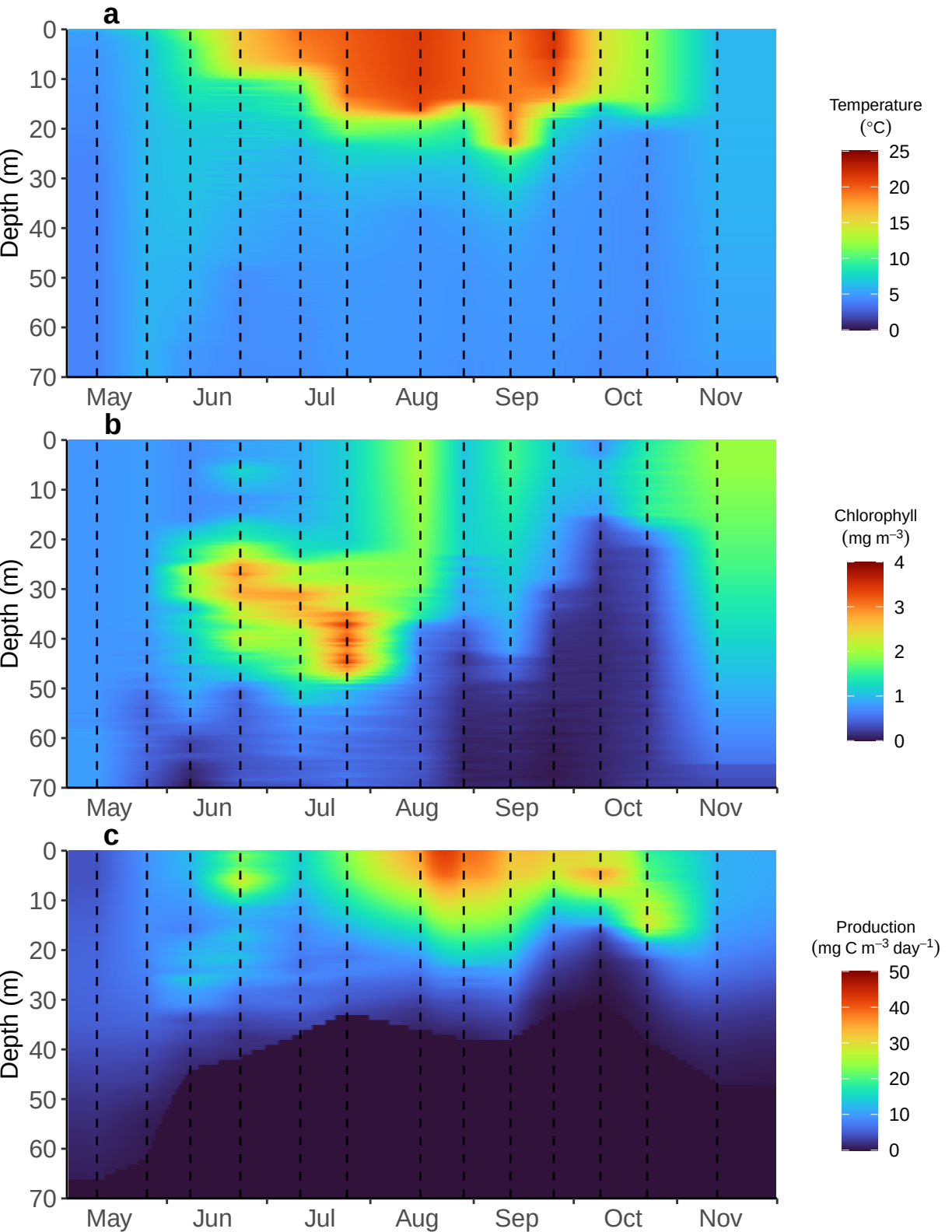
a
b
c
Depth (m)
0
10
20
30
40
50
60
70
May
Jun
Jul
Aug
Sep
Oct
Nov
Temperature
(°C)
25
20
15
10
5
0
Chlorophyll
(mg m−3)
4
3
2
1
0
Production
(mg C m−3 day−1)
50
40
30
20
10
0

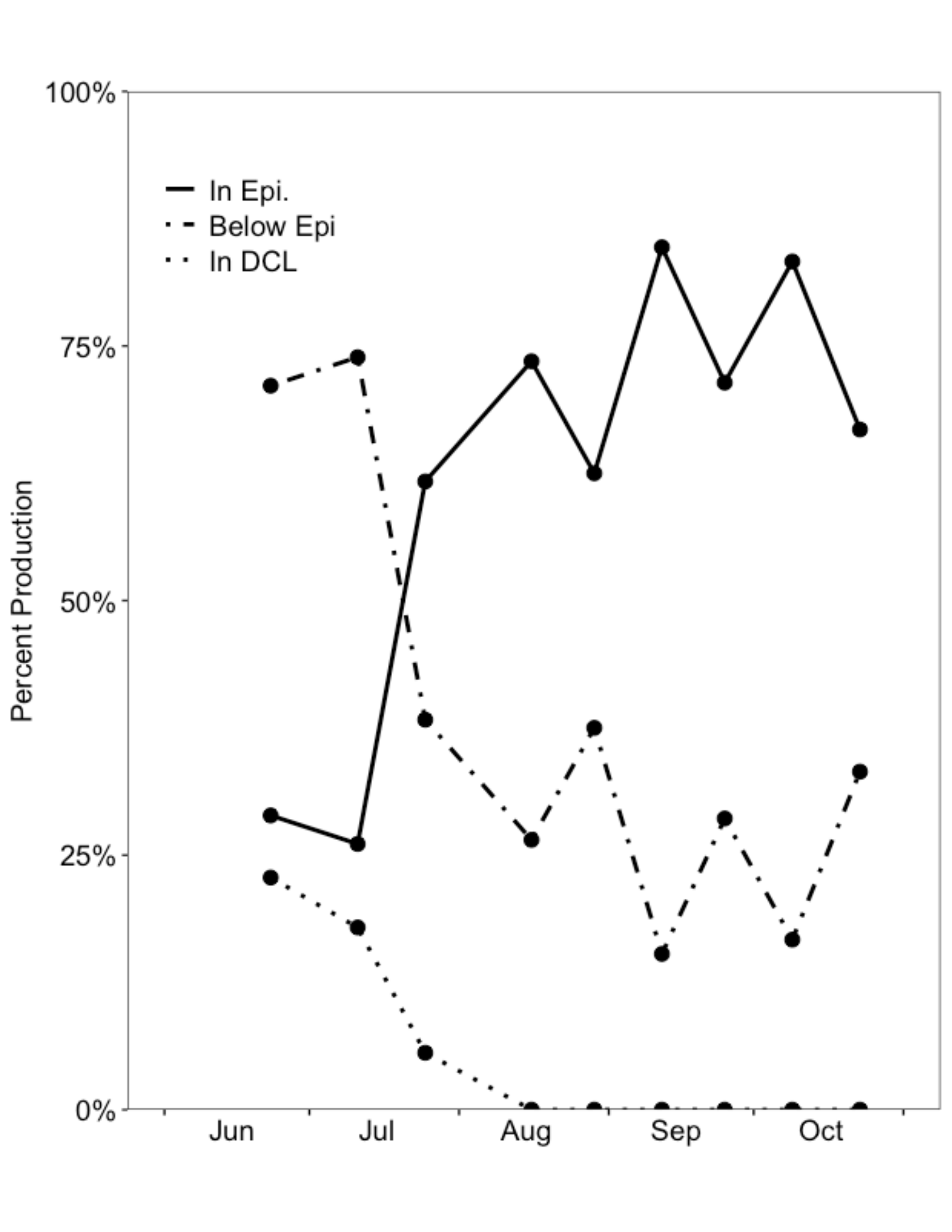
100%
75%
50%
25%
0%
Percent Production
In Epi.
Below Epi
In DCL
Jun
Jul
Aug
Sep
Oct

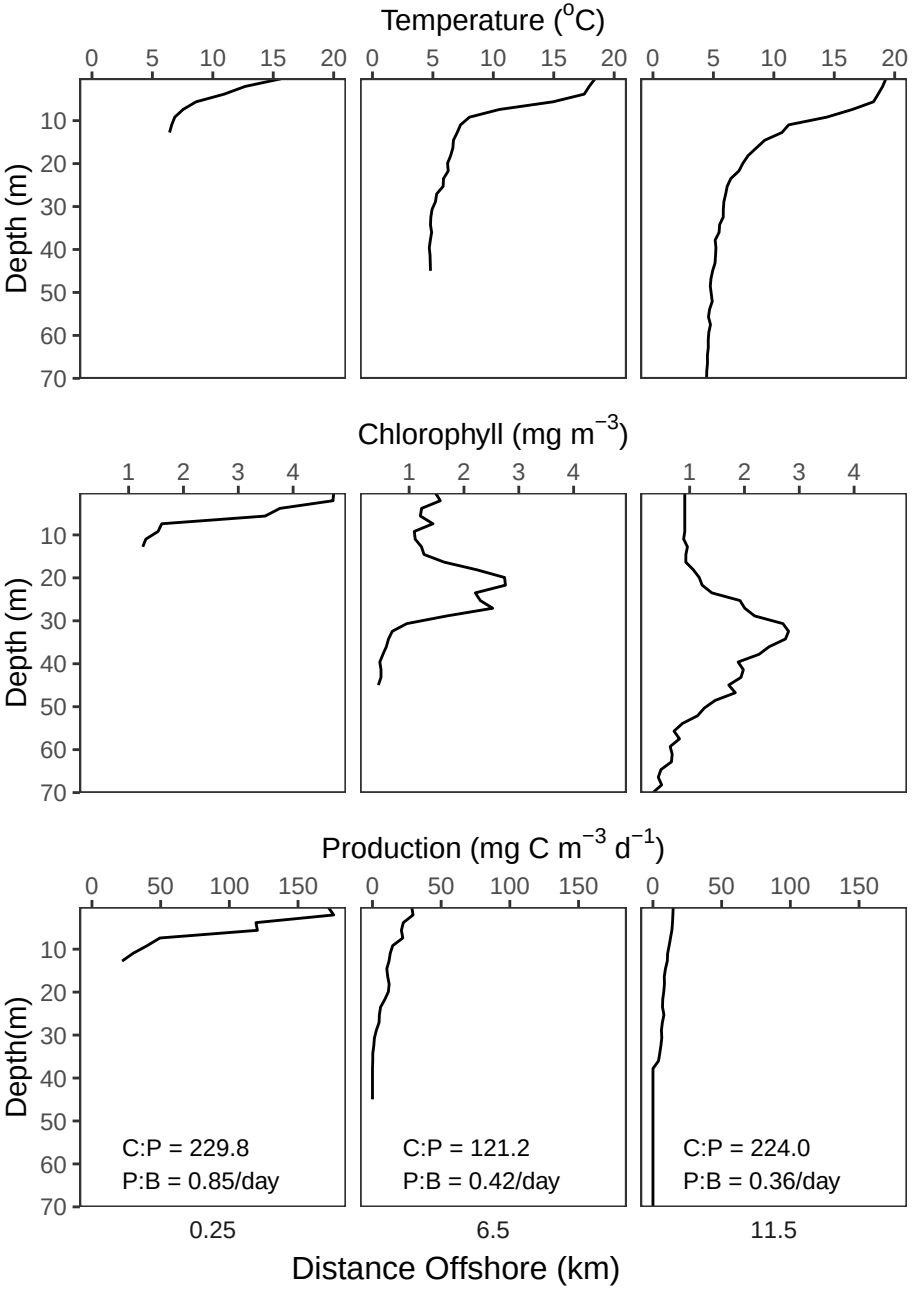
Temperature (°C)
0 5 10 15 20
Depth (m)
10 20 30 40 50 60 70
Chlorophyll (mg m−3)
1 2 3 4
Production (mg C m−3 d−1)
0 50 100 150
Depth(m)
C:P = 229.8
P:B = 0.85/day
C:P = 121.2
P:B = 0.42/day
C:P = 224.0
P:B = 0.36/day
0.25
6.5
11.5
Distance Offshore (km)

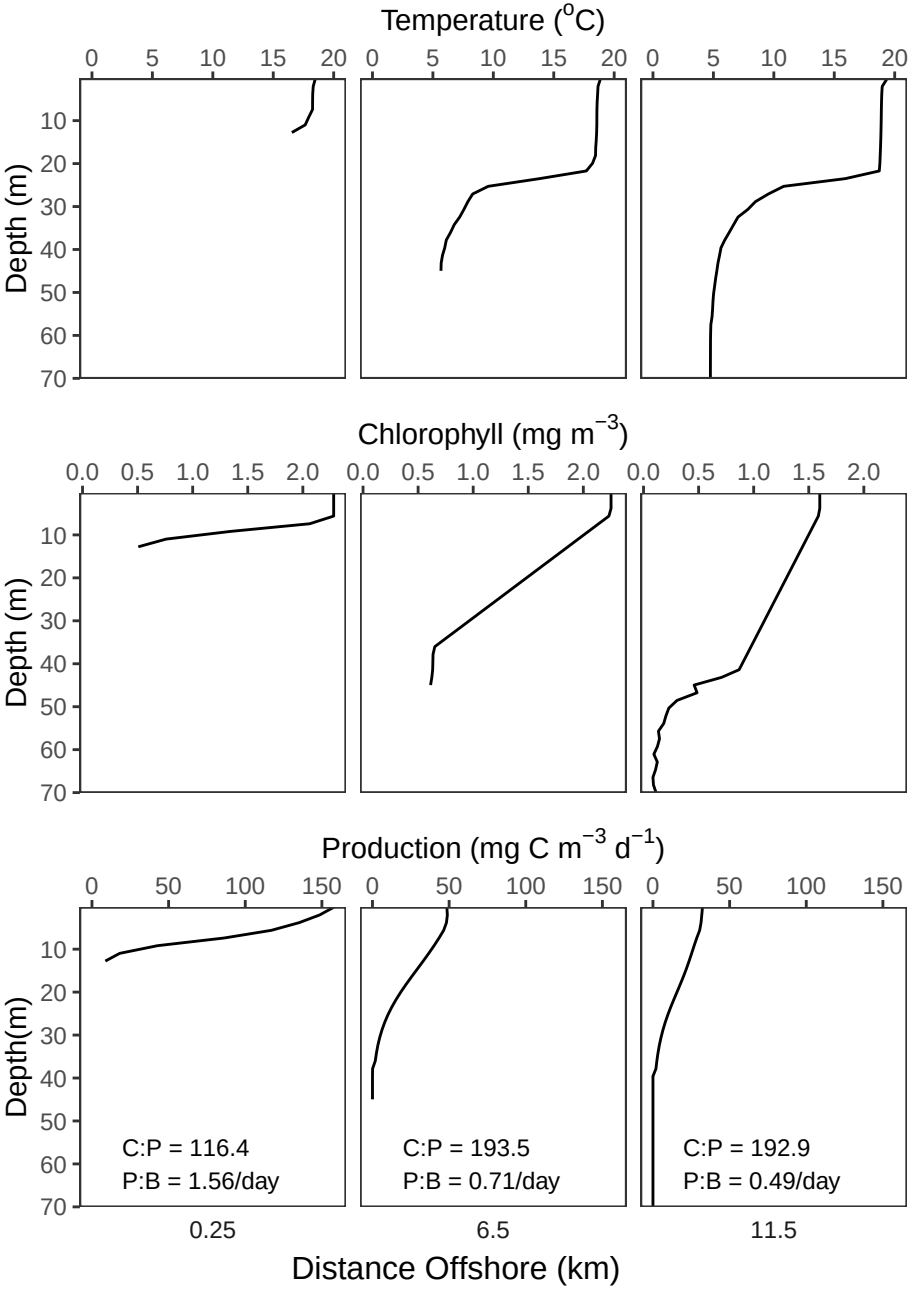
Temperature (°C)
0 5 10 15 20
Depth (m)
10 20 30 40 50 60 70
Chlorophyll (mg m−3)
0.0 0.5 1.0 1.5 2.0
Production (mg C m−3 d−1)
0 50 100 150
Depth(m)
C:P = 116.4
P:B = 1.56/day
C:P = 193.5
P:B = 0.71/day
C:P = 192.9
P:B = 0.49/day
0.25
6.5
11.5
Distance Offshore (km)

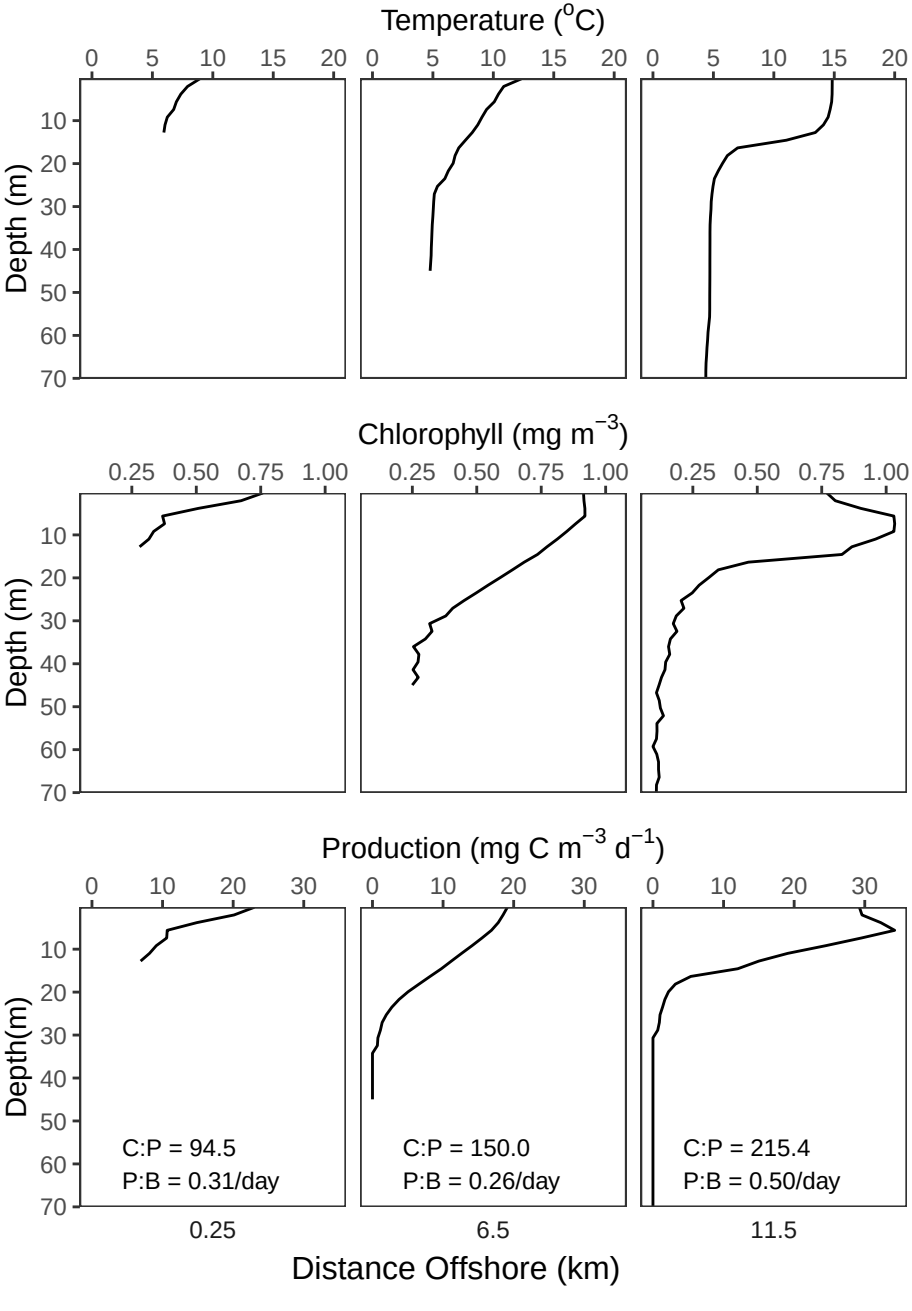
Temperature (°C)
0 5 10 15 20
Depth (m)
10 20 30 40 50 60 70
Chlorophyll (mg m−3)
0.25 0.50 0.75 1.00
Production (mg C m−3 d−1)
0 10 20 30
Depth(m)
C:P = 94.5
P:B = 0.31/day
C:P = 150.0
P:B = 0.26/day
C:P = 215.4
P:B = 0.50/day
0.25
6.5
11.5
Distance Offshore (km)

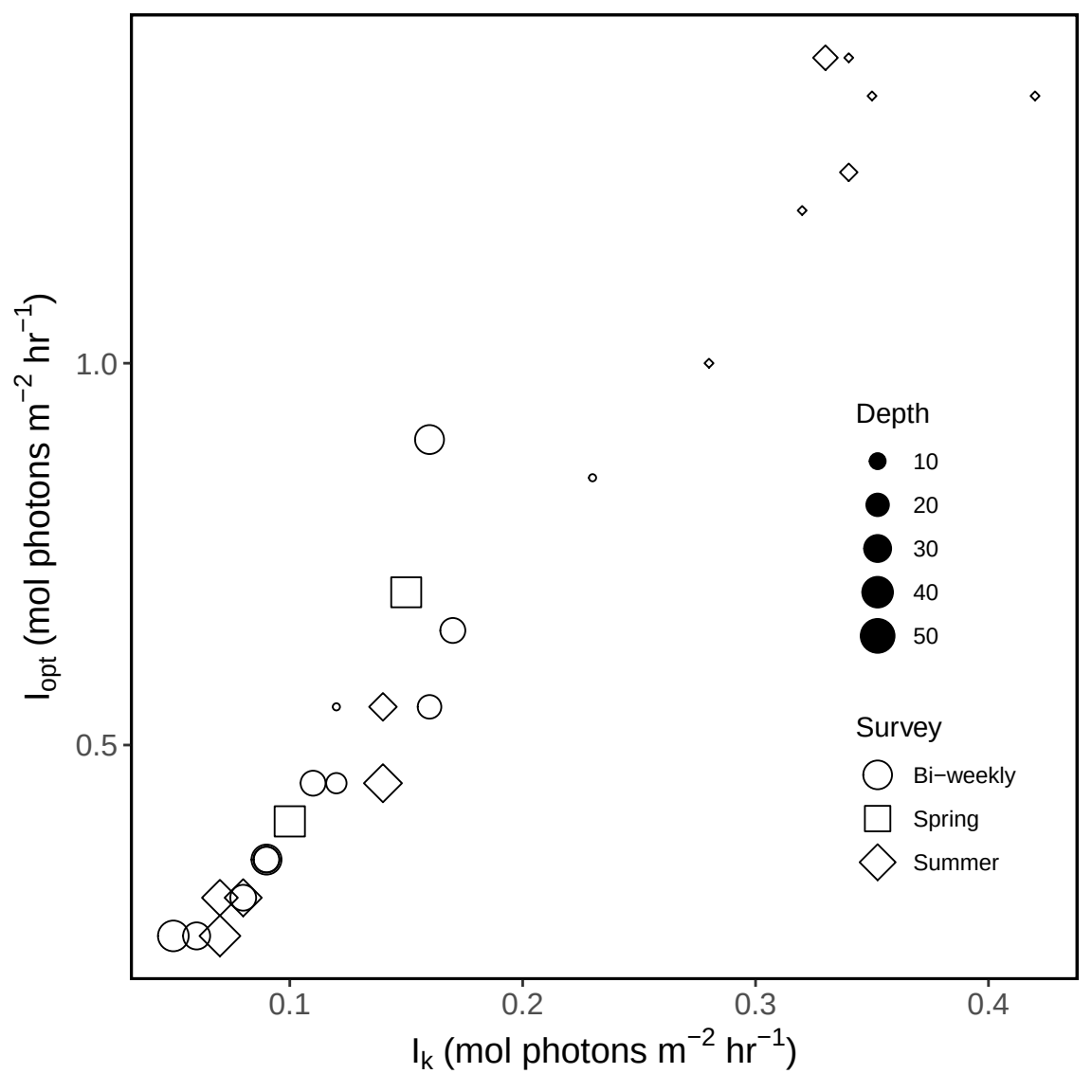
1.0
0.5
0.1
0.2
0.3
0.4
I_{opt} (mol photons m^{-2} hr^{-1})
I_k (mol photons m^{-2} hr^{-1})
Depth
10
20
30
40
50
Survey
Bi−weekly
Spring
Summer